Alonzo Kelly

Robotics Institute
Carnegie Mellon University
Pittsburgh, PA 15213-3890, USA
alonzo@ri.cmu.edu
http://www.frc.ri.cmu.edu/~alonzo

Linearized Error Propagation in Odometry

Abstract

The related fields of mobile robotics and ground vehicle localization lack a linearized theory of odometry error propagation. By contrast, the equivalent Schuler dynamics which apply to inertial guidance have been known and exploited for decades. In this paper, the general solution of linearized propagation dynamics of both systematic and random errors for vehicle odometry is developed and validated. The associated integral transforms are applied to the task of eliciting the major dynamic behaviors of errors for several forms of odometry. Interesting behaviors include path independence, response to symmetric inputs, zeros, extrema, monotonicity and conservation. Applications to systems theory, systems design, and calibration are illustrated.

KEY WORDS—mobile robots, odometry, error propagation, calibration, position estimation, localization, dead reckoning

1. Introduction

For the purpose of this paper, odometry will be defined as dead reckoning from indications of linear velocity with respect to the frame of reference of interest. Inertial navigation differs from odometry slightly by its use of linear acceleration indications, and more profoundly by its use of inertially referenced indications.

Odometry is also materially distinct from triangulation based position fixing. Triangulation errors are algebraic expressions—exhibiting no dynamics. Odometry and its errors evolve according to differential equations whose solutions are integrals.

This essentially dynamic nature of odometry error propagation is unavoidable, and a significant inconvenience. As a result, the problem of analytically computing the navigational error expected in odometry from a given set of sensor errors on a given trajectory has remained both a fundamental and an unsolved problem.

This paper addresses the problem of understanding the relationship between errors present in sensor indications in odometry, and the resultant error in computed vehicle pose. Analytical rather than numerical results are targeted. While a numerical solution to the problem of computing the resultant error is trivial, symbolic solutions yield dividends in the form of understanding the general case that numerical ones cannot.

1.1. Motivation

This work is motivated by a recurrent set of questions which arise for position estimation systems in mobile robots. Historically they have been answered numerically or in an ad hoc manner. How good do the sensors need to be? What kind of localization error can be expected if this particular sensor is used? Under what conditions do errors cancel out? What is the best way to calibrate the systematic or stochastic error model of this sensor?

The integral transforms derived here encapsulate the path-dependent dynamic effects once the character of the trajectory is fixed. These moments thereby enable rapid analytical solutions to many of the design questions posed above.

A personal motivation for this work relates to several counter-intuitive phenomena which have been observed on mobile robot odometry systems. For the robots shown in Figure 1, behaviors observed include:

- odometry error (using a good gyro) at the point of closure of a 1 km trajectory as low as 1/10% of distance traveled;

- the ability to reverse the effect of some sources of error by driving backward over the path which accumulated them;

- the existence of an optimal update rate in an odometry aided visual tracker.

1.2. Prior Work

The aerospace guidance community has enjoyed the benefits of a theoretical understanding of error propagation for
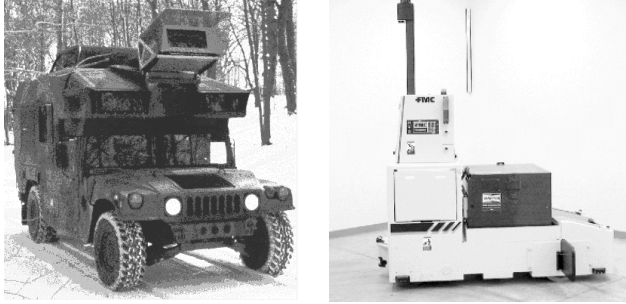
Fig. 1. Robots whose interesting odometry error behaviors have motivated this work. The HMMWV odometry was excellent on rough terrain on closed paths. The AGV had errors whose effects could be reversed by driving backwards.

Fig. 2. Coordinates for odometry.

at least five decades (Pinson 1963). In inertial guidance, the governing differential equations and their solutions have long since been relegated to textbooks (Britting 1971; Brown and Hwang 1996). It is well known that, in the presence of gravity, most horizontal errors exhibit oscillation with the characteristic Schuler period of 84 min while the vertical channel is rendered unstable.

Likewise, the essentially geometric nature of satellite navigation system error relationships has been known since before the GPS satellites were in operation (Milliken and Zoller 1978). Using the Kalman filter, applied earliest to shipborne inertial systems (Bona and Smay 1966), the theoretical propagation of error, at least in numerical form, has been an essentially solved problem.

Robotics embraced these results several decades later (Smith and Cheeseman 1986; Durrant-Whyte 1987). However, the guidance community seems not to have provided the relevant analytical results for the land navigation systems which are typical of mobile robots: assemblies of wheel encoders, compasses, gyros, etc.

Analytical study of error propagation in mobile robot odometry appears only rarely in the literature. Early work in Wang (1988) concentrates on improving estimates for a single iteration of the estimation algorithm by incorporating knowledge of the geometry of the path followed between odometry updates. In Borenstein and Feng (1995), a geometric method is presented for the calibration of certain systematic errors on rectangular closed trajectories. In Chong and Kleeman (1997), a recurrence equation solution is obtained for non-systematic error on constant curvature trajectories. In Nettleton, Gibbens, and Durrant-Whyte (2000), a closed-form solution for a broader optimal estimation problem is presented. This paper presents the general solution for linearized systematic and random error propagation in odometry for any trajectory or error model.
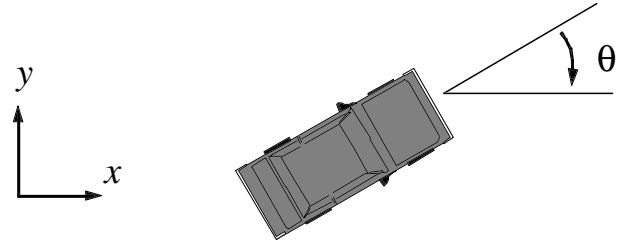
1.3. Problem Description

Odometry is a form of dead reckoning because the available measurements must be integrated to provide a navigation solution. In the common "forced dynamics" formulation of odometry, the measurements, normally denoted $\underline{z}(t)$, are identified with the usual control inputs $\underline{u}(t)$—the measurements act as a forcing function.

If the state vector $\underline{x}(t)$ and input vector $\underline{u}(t)$ are chosen to be

$$\underline{x}(t) = \begin{bmatrix} x(t) & y(t) & \theta(t) \end{bmatrix}^T \quad \underline{u}(t) = \begin{bmatrix} V(t) & \omega(t) \end{bmatrix}^T \quad (1)$$

then, the associated odometry equations are those of the "integrated heading" case:

$$\frac{d}{dt} \begin{bmatrix} x(t) \\ y(t) \\ \theta(t) \end{bmatrix} = \begin{bmatrix} V(t)\cos\theta(t) \\ V(t)\sin\theta(t) \\ \omega(t) \end{bmatrix}. \quad (2)$$

The x-axis has been implicitly chosen as the heading datum as illustrated in Figure 2.

Many alternative formulations of odometry are possible. This one and many others have the key properties of being homogeneous in the inputs, nonlinear in the states, and reduced to echelon form. Due to the latter property, the solution is immediate:

$$\theta(t) = \theta(0) + \int_0^t \omega(t)dt$$

$$x(t) = x(0) + \int_0^t V(t)\cos\theta(t)dt \quad (3)$$

$$y(t) = y(0) + \int_0^t V(t)\sin\theta(t)dt.$$

Closed-form solutions to these equations are nevertheless available only for the simplest of inputs and nonlinear error propagation is equally intractable.

This paper addresses the following problem. Let the inputs (or equivalently, the sensors) to the system be corrupted by additive errors $\delta \underline{u}(t)$ as follows:

$$\underline{u}'(t) = \underline{u}(t) + \delta \underline{u}(t). \tag{4}$$

Using these input errors and the system dynamics, determine the behavior of the associated errors in the computed vehicle pose:

$$x'(t) = x(t) + \delta x(t)$$
$$y'(t) = y(t) + \delta y(t) \tag{5}$$
$$\theta'(t) = \theta(t) + \delta \theta(t).$$

The errors can be systematic or random in nature, and solutions for either case are sought.

1.4. Error Models

It must be emphasized at the outset that while the problem of determining the form of error models which are representative of reality is a central and an important one, such is not the purpose of this paper. Here, the quest is for the mathematical expressions which map models of sensor errors onto values for the generated vehicle pose errors. Only sufficiently correct sensor error models, however, will generate sufficiently correct pose errors.

To the degree that the results derived here are used for the purposes of calibration, the reader should be wary that any model can be fit to any data, and the justification of the model used is an important step in the calibration process.

1.5. Methodology

In broad terms, the approach employed, is as follows.

- Following common practice, convert the estimation problem into an equivalent control problem by identifying the measurements $\underline{z}(t)$ with the system inputs $\underline{u}(t)$.

- Linearize the system dynamics. Apply linear systems theory to this equivalent linear control problem.

- Exploit a commutativity property of the associated system Jacobian which provides an explicit expression for the transition matrix, even when the linearized dynamics are time-varying. Accordingly, write the transition matrix in terms of the matrix exponential.

- Exploit the upper triangularity of the associated system Jacobian (which results from the echelon form of the original equations) to easily sum the more generally infinite matrix series.

- Write the solution integrals for both deterministic and stochastic cases to generate the general linearized solutions.

- For concrete examples, substitute error models and trajectories in order to generate specific solutions to specific cases; a straight line, a pure rotation, and a constant curvature arc are illustrated.

- Demonstrate the use of the resulting theory in several applications.

- Verify the resulting equations and the validity of linearization through comparison with direct numerical integration of the nonlinear equations on a trajectory of general shape.

1.6. Notational Conventions

Most of the notation used in subsequent sections follows that used in the classical texts such as Stengel (1994). In particular, the operator δ will be used to signify perturbation (systematic or random) and a fairly standard set of conventions of linear systems theory and optimal estimation will be used. The tilde diacritical mark "$\sim$" above a symbol indicates that it is in some way derived from the associated symbol which lacks this mark.

Capital letters signify matrices, underlined lowercase indicates a vector and other lowercase letters are scalars.

1.7. General Form

In the most general case, the odometry problem takes the abstract form:

$$\underline{\dot{x}}(t) = \underline{f}[\underline{x}(t), \underline{u}(t), \underline{p}] \tag{6}$$

for some nonlinear function $\underline{f}()$, state vector $\underline{x}(t)$, input vector $\underline{u}(t)$ and parameter vector $\underline{p}$. It is also useful at times to add an observer equation which permits the input to be overdetermined:

$$\underline{z}(t) = h[\underline{x}(t), \underline{u}(t), \underline{p}]. \tag{7}$$

This equation could be used to model, for example, a situation where encoders are provided on four wheels even though two are enough to determine position and heading. the parameter vector would include, for example the positions of the sensors with respect to the reference frame whose pose is being computed.

Many texts use a separate symbol, such as $\underline{w}(t)$, to distinguish random inputs from deterministic ones. Here, the input $\underline{u}(t)$ will refer to either as the case requires.

1.8. Treatment of Parameters

Note that while the distinction between state $\underline{x}(t)$ and input $\underline{u}(t)$ is fundamental, the distinction between input and parameter $\underline{p}$ is not. Parameters will henceforth be absorbed into the input vector and the vector $\underline{p}$ will be dropped from lists of function arguments. Parameters will be interpreted as inputs which happen to be time invariant. This device simplifies notation and clarifies thinking. For while parameters are normally considered time invariant, their errors may not be. Wheelbase, for example, is nominally constant but tire deformations lead to time-varying errors in wheelbase.

For later reference, the generic nonlinear system with observer now takes the form:

$$\dot{\underline{x}}(t) = \underline{f}[\underline{x}(t), \underline{u}(t)]$$
$$\underline{z}(t) = h[\underline{x}(t), \underline{u}(t)]. \tag{8}$$

2. Relevant Properties of Nonlinear Systems

It is easy to see that substituting eq. (4) into eq. (3) generates equations with little hope of solution, although the simple cases of a zero curvature and constant curvature trajectory are solvable. Nonetheless, some important properties of odometry can be discerned without solving the nonlinear equations. These and many more can also be observed in the linearized solution integrals.

This section outlines some important properties of both the system dynamics and the reference trajectory which evoke interesting behaviors in error propagation.

2.1. Implications of Homogeneity

When the nonlinear dynamics satisfy

$$\underline{f}[\underline{x}(t), k \times \underline{u}(t)] = k^n \times \underline{f}[\underline{x}(t), \underline{u}(t)] \tag{9}$$

for some constant k, the system is said to be homogeneous of degree n with respect to $\underline{u}(t)$. Homogeneity implies that $\underline{u}(t)$ must occur inside $f()$ solely in the form of a factor of its nth power:

$$\underline{f}[\underline{x}(t), \underline{u}(t)] = \underline{u}^n(t) g(\underline{x}(t)). \tag{10}$$

As a result, all terms of the Taylor series of $f()$ over $\underline{u}(t)$ of order less than n vanish. When they do it has important implications.

Different forms of odometry are often homogeneous (actually linear) with respect to inputs. Based on the following discussion, it can be shown that odometry itself is memoryless, reversible, regular, and motion-dependent. Intuitively, motion stops instantly when the velocity is zeroed, and driving backwards causes the solution to play back in reverse.

Later analysis will uncover these and more interesting behaviors in the linearized solutions for error propagation. By

definition, a linearized error propagation solution is homogeneous to the first degree in its error inputs. The more interesting questions are why is linearized random error never reversible and when is systematic error reversible with respect to input linear velocity as well as errors.

2.1.1. Memoryless

Systems which are homogeneous to any non-zero degree with respect to their inputs are memoryless—their zero input response is zero—so they can be stopped instantly by nulling the inputs. It is not necessarily the case that $f()$ is independent of the states (i.e., the system has no dynamics) because the states may be multiplied by the inputs (as they are in odometry) to create homogeneity.

2.1.2. Reversibility and Monotonicity

Systems of odd degree homogeneity are odd with respect to $\underline{u}(t)$ and hence reversible because they can be driven precisely back over their original trajectory with little effort by simply reversing the input signal $\underline{u}(t)$ in time. Systems of even degree homogeneity are even with respect to $\underline{u}(t)$ and monotone because the sign of the state derivative is invariant under changes in the inputs.

2.1.3. Regularity

If a system is homogeneous with respect to a particular input $u_i(t)$ that can be written as the time rate of some other parameter such as s, it can also be divided by the input without creating a singularity:

$$\frac{\underline{f}[\underline{x}(t), \underline{u}(t)]}{u_i(t)} = \frac{f[\underline{x}(t), \underline{u}(t)]}{(ds)/(dt)} = finite. \tag{11}$$

Hence, a change of variable becomes possible and the system can be written in the form:

$$\frac{d}{ds}\underline{x}(s) = \tilde{\underline{f}}[\underline{x}(s), \underline{u}(s)]. \tag{12}$$

Borrowing (and slightly changing) a term from differential geometry, such well-behaved systems can be referred to as regular.

2.1.4. Motion Dependence

Regular systems are motion-dependent because the state advances only under non-zero velocity conditions. The distinction is important in odometry because the influence of inertially derived sensor errors (inertial navigation) continues to grow when motion stops, whereas that of sensor errors for terrain relative indications (odometry) does not.

2.2. Implications of Trajectory Closure

State space trajectories which close on themselves are of special interest in error analysis. In general, a trajectory closes on the interval [0, T] when the closure condition is satisfied by the state space trajectory:

$$\underline{x}(T) - \underline{x}(0) = \int_0^T F[\underline{u}(t)]dt = 0. \tag{13}$$

In a general solution, the integrand $F(\ )$ will depend on the inputs but not the state. The closure condition places no other constraints on the trajectory other than that it form a closed loop; trajectories of arbitrary shape may satisfy it. Nonetheless, two special cases are important for error analysis.

2.2.1. Symmetry

Symmetry is the case where the integrand is symmetric (e.g. periodic or aperiodic) in time or it can be converted to one which is symmetric in space and the bounds of integration are just right. If it is possible to partition the interval of integration such that every time t_1 can be paired one-to-one with another time t_2 such that

$$F[\underline{u}(t_1)]dt = -F[\underline{u}(t_2)]dt \tag{14}$$

then the closure condition will be satisfied. Symmetry is a property of the state derivative and indirectly a property of the inputs because only certain inputs produce symmetric state derivatives of the right period to generate trajectory closure. Such integrals are relevant here because they provide the conditions for which odometry error must cancel on closed trajectories of particular shape.

2.2.2. Path Independence

Whereas symmetry is a path property, path independence is a system property. When the integrand can be cast as a potential, (for example, over input space), then a closed path (for example, in input space) generates a closed path in state space.

The example case can be written in the form

$$\underline{F}[\underline{u}(t)]dt = \frac{\partial}{\partial \underline{u}}\underline{\xi}(\underline{u}) \cdot d\underline{u} = d\underline{\xi}(\underline{u}) \tag{15}$$

where the middle expression is a Jacobian matrix of some potential $\underline{\xi}$ over the input. The resulting total differential can be integrated in closed form to produce the solution:

$$\underline{x}(t) = \underline{\xi}[\underline{u}(t)]. \tag{16}$$

These systems are path-independent; the state is dependent only on the present value of the input rather than its history. Such integrals are relevant here because they provide the conditions for which odometry error must cancel on closed trajectories of any shape.

2.2.3. Path Independence of Velocity Scale Error

It is possible to show that odometry error due to velocity (e.g., encoder) scale errors is independent of path. This property follows from odometry's homogeneity in velocity. If linear velocity is corrupted by additive scale errors (while angular velocity is unchanged) as follows

$$V'(t) = V(t) + \delta V(t) = V(t) + \alpha V(t) \quad \theta'(t) = \theta(t)$$

then the perturbed position vector must vanish on a closed path:

$$\int_0^t \begin{bmatrix} c\theta' \\ s\theta' \end{bmatrix} V'(t)dt = (1 + \alpha) \int_0^t \begin{bmatrix} c\theta \\ s\theta \end{bmatrix} V(t)dt$$
$$\oint \begin{bmatrix} c\theta' \\ s\theta' \end{bmatrix} V'(t)dt = (1 + \alpha) \oint \begin{bmatrix} dx \\ dy \end{bmatrix} = 0. \tag{17}$$

Intuitively, position coordinates are path-independent by definition and any error which scales the path uniformly preserves this property. Note that it was not necessary to solve the nonlinear dynamics to reach this conclusion and that the derivation fails when heading angle θ is also corrupted by a time-varying error.

3. Linearized Error Dynamics

Here, the governing equations of odometry error dynamics are developed and described.

3.1. Linearization

Perturbative techniques linearize nonlinear dynamical systems in order to study their first-order behavior. As long as errors are small, the perturbative dynamics are a good approximation to the exact behavior, and they can be far more illuminating.

With reference to eq. (8), several Jacobian matrices are defined which may depend on the state and the input, and are evaluated on some reference trajectory:

$$F(t) = \frac{\partial}{\partial \underline{x}}\underline{f}\bigg|_{\underline{x},\underline{u}} \quad G(t) = L(t)\frac{\partial}{\partial \underline{u}}\underline{f}\bigg|_{\underline{x},\underline{u}}$$
$$H(t) = \frac{\partial}{\partial \underline{x}}\underline{h}\bigg|_{\underline{x},\underline{u}} \quad M(t) = N(t)\frac{\partial}{\partial \underline{u}}\underline{h}\bigg|_{\underline{x},\underline{u}}. \tag{18}$$

To be consistent with common notation, $G(t)$ will be used when discussing systematic error and $L(t)$ will be used when discussing random error. $M(t)$ and $N(t)$ will be used similarly.

Equation (8) is now linearized as follows:

$$\delta\underline{\dot{x}}(t) = F\{\underline{x}(t), \underline{u}(t)\}\delta\underline{x}(t) + G\{\underline{x}(t), \underline{u}(t)\}\delta\underline{u}(t)$$
$$\delta\underline{z}(t) = H\{\underline{x}(t), \underline{u}(t)\}\delta\underline{x}(t) + M\{\underline{x}(t), \underline{u}(t)\}\delta\underline{u}(t). \tag{19}$$

Subsequently, the notational dependence of the Jacobians on the state and the input will be suppressed for brevity but all of these matrices will generally depend on both. Although eq. (19) may still be nonlinear in the state and the input, it is linear in the perturbations. The first is the linear perturbation equation and the second is the linearized observer. These provide a linear approximation to the propagation of systematic error as well as a description for the propagation of the mean of random error.

If the errors $\delta \underline{u}(t)$ are random in nature, eq. (19) is often used in a heuristic sense in stochastic calculus because direct integration of random signals is beyond the scope of traditional calculus (Maybeck 1982).

3.2. Deterministic Case

For deterministic error, the linearized dynamics take the form:

$$\delta \dot{\underline{x}}(t) = F(t)\delta \underline{x}(t) + G(t)\delta \underline{u}(t)$$
$$\delta \underline{z}(t) = H(t)\delta \underline{x}(t) + M(t)\delta \underline{u}(t). \quad (20)$$

If $\delta \underline{u}(t)$ is not known directly but $\delta \underline{z}(t)$ is (for example, when wheel velocities are measured but axle velocity is the input), the linearized observer equation (20) can be solved for $\delta \underline{u}(t)$ by first writing:

$$M(t)\delta \underline{u}(t) = \delta \underline{z}(t) - H(t)\delta \underline{x}(t).$$

The case where the inputs are underdetermined is not useful here. In the event that the measurements determine or overdetermine the inputs, the left pseudo-inverse applies:

$$M^L = \left[M^T(t)M(t) \right]^{-1} M^T(t), \quad (21)$$

solving

$$\delta \underline{u}(t) = M^L \left[\delta \underline{z}(t) - H(t)\delta \underline{x}(t) \right]. \quad (22)$$

This is the input which minimizes the residual between the actual observations and those that would be predicted from the state and the inputs:

$$\delta \underline{z}(t) - \left[H(t)\delta \underline{x}(t) + M(t)\delta \underline{u}(t) \right].$$

Substituting this back into the state perturbation equation gives

$$\delta \dot{\underline{x}}(t) = F(t)\delta \underline{x}(t) + G(t) \left\{ M^L[\delta \underline{z}(t) - H(t)\delta \underline{x}(t)] \right\},$$

which reduces to

$$\delta \dot{\underline{x}}(t) = \left\{ F(t) - G(t)M^L H(t) \right\} \delta \underline{x}(t) + G(t)M^L \delta \underline{z}(t). \quad (23)$$

This is of the same form as the original perturbation equation with modified matrices and the measurements acting as the input:

$$\delta \dot{\underline{x}}(t) = \tilde{F}(t)\delta \underline{x}(t) + \tilde{G}(t)\delta \underline{z}(t). \quad (24)$$

In this way, the observer equation can be substituted into the dynamics to preserve the original forced dynamics form. It can be dispensed with for the balance of the article and the deterministic case can be considered to be defined by the linear perturbation equation:

$$\delta \dot{\underline{x}}(t) = F(t)\delta \underline{x}(t) + G(t)\delta \underline{u}(t). \quad (25)$$

Once the matrices are filled in, it is instructive to evaluate the resulting equations for homogeneity with respect to both the system inputs and the error inputs.

3.3. Stochastic Case

For practical treatment of random errors, the second moment or "covariance" of the error is considered and the state covariance and input spectral density matrices are defined:

$$P = \text{Exp}(\delta \underline{x}(t)\delta \underline{x}(t)^T)$$
$$Q = \text{Exp}(\delta \underline{u}(t)\delta \underline{u}(t)^T)\delta(t - \tau). \quad (26)$$

In the second case the Dirac delta $\delta(t - \tau)$ signifies that the random sequence $\delta \underline{u}(t)$ is white and that the units of Q are the time rate of covariance. Covariance is the stochastic equivalent of a linearized deterministic error description. To express its propagation over time, an expression for P must be differentiated, or the expectation and derivative of an expression for $\delta \underline{x}(t)$ must be performed. The result is derived in several texts including Gelb (1974) and it is known as the linear variance equation:

$$\dot{P}(t) = F(t)P(t) + P(t)F(t)^T + L(t)Q(t)L(t)^T$$
$$R(t) = H(t)P(t)H(t)^T + M(t)Q(t)M(t)^T. \quad (27)$$

Given a forced dynamics formulation it is consistent to assume that the process noise is known, because the process inputs are really the measurements, and known measurement statistics are a fundamental assumption of this work. This assumption is not the standard assumption of a state space Kalman filter, so the following derivation is peculiar to the forced dynamics formulation.

Define:

$$R = \text{Exp}\left(\delta \underline{z}(t)\delta \underline{z}(\tau)^T \right) \delta(t - \tau).$$

If the statistics of $\delta \underline{u}(t)$ are not known directly but those of $\delta \underline{z}(t)$ are, the measurement (process) covariance Q can be written in terms of the covariance in the observations R and the state P. Taking the second moment of eq. (20) and suppressing the time dependence notation temporarily:

$$R = \text{Exp}\left\{ \delta \underline{z}\delta \underline{z}^T \right\}$$
$$= \text{Exp}\left\{ \left[H\delta \underline{x} + N\delta \underline{u} \right] \left[H\delta \underline{x} + N\delta \underline{u} \right]^T \right\}.$$

If the process noises are (as commonly assumed) uncorrelated with the state noise, this is

$$R = HPH^T + NQN^T.$$

This matrix equation can be solved for Q to yield

$$Q = \left[N^T \left[R - HPH^T \right]^{-1} N \right]^{-1}.$$

Substituting this into the linear variance equation gives

$$\dot{P} = FP + PF^T + L \left[N^T \left[R - HPH^T \right]^{-1} N \right]^{-1} L^T.$$

When N is square this becomes

$$\dot{P} = FP + PF^T + LN^{-1}RN^{-T}L^T$$
$$- LN^{-1}HPH^T N^{-T}L^T$$

and when H is the zero matrix (measurements related to inputs, not states), this is

$$\dot{P} = FP + PF^T + LN^{-1}RN^{-T}L^T.$$

This is of same form as the original variance equation with modified matrices and the measurements acting as the input:

$$\dot{P}(t) = F(t)P(t) + P(t)F(t)^T + L(t)\tilde{Q}(t)L(t)^T$$

where

$$\tilde{Q}(t) = N^{-1}RN^{-T}. \tag{28}$$

In this way, the observer equation can be substituted into the dynamics to preserve the original forced dynamics form. Again, it can be dispensed with; for the balance of the article the stochastic case can be considered to be defined by the linear variance equation:

$$\dot{P}(t) = F(t)P(t) + P(t)F(t)^T + L(t)Q(t)L(t)^T. \tag{29}$$

4. Solution Basis of Linearized Systems

Linearized systems satisfy superposition by definition. Accordingly, linear error dynamics solutions can be profitably described in terms of a sum of contributions—each of which is traceable to a single input error source.

4.1. General Solutions

The equations to be solved are eqs. (25) and (29). It is well known that the solution to these equations rests on the knowledge of a very important matrix called the transition matrix, denoted $\Phi(t, \tau)$. One definition for this matrix is that it is the solution to:

$$\frac{d}{dt}\Phi(t, \tau) = F(t)\Phi(t, \tau). \tag{30}$$

The general solutions for the propagation of systematic and random error are respectively of the form of the vector and matrix convolution integrals:

$$\delta\underline{x}(t) = \Phi(t, t_0)\delta\underline{x}(t_0) + \int_{t_0}^{t} \Phi(t, \tau)G(\tau)\delta\underline{u}(\tau)d\tau$$

$$P(t) = \Phi(t, t_0)P(t_0)\Phi^T(t, t_0) \tag{31}$$

$$+ \int_{t_0}^{t} \Phi(t, \tau)L(\tau)Q(\tau)L^T(\tau)\Phi^T(t, \tau)d\tau.$$

The first also describes the evolution of bias $\delta\underline{x}(t)$ in the state due to a biased random input of mean $\delta\underline{u}(t)$. Once a trajectory and an error model are assumed, the only unknown in both of these equations is the transition matrix.

4.1.1. Error Propagation Behavior

Some important behaviors of error propagation are evident from the structure of these solutions. Both solutions consist of a state (initial conditions $\underline{x}(t_0)$ or $P(t_0)$) response and an input ($\delta\underline{u}(\tau)$ or $Q(\tau)$) response. The state response is always path independent (because it is not an integral) and hence it vanishes on any closed trajectory. Both general solutions can exhibit extrema and even zeros.

Although the input response may be path-independent or otherwise vanish under conditions of symmetry, it is in general, path-dependent. In other words, error propagation is a functional defined on the inputs and it can, in certain cases, be expressed as a functional on the reference state space trajectory.

4.1.2. Input Transition Matrix

It is useful to define the (potentially non-square) input transition matrix as

$$\tilde{\Phi}(t, \tau) = \Phi(t, \tau)L(\tau) = \Phi(t, \tau)G(\tau). \tag{32}$$

Based on the form of the above solutions, this matrix clearly maps a given systematic or random error at time τ onto its net effect on the state error occurring later at time t. In effect, linearization for the purposes of studying error propagation amounts to treating errors occurring at different times independently of each other, their compounded effects being second order. This matrix will shortly be exposed as the essential matrix of odometry error propagation. For each form of odometry, it captures the effects of both system dynamics and input measurement errors.

4.2. Error Moment Matrices

It is instructive to isolate the components of output error which can be traced to each individual source of input error. For

linearized systems, the total solution can be expected to be the superposition of all such components. Indeed, a set of basis vectors and matrices can be derived for systematic and random error, respectively, based only on the input transition matrix.

4.2.1. Influence Matrices

Let $\underline{\tilde{\Phi}}_i$ denote the ith column of the input transition matrix. It is easy to show (for example, by temporarily zeroing all elements but one) that for a given element δu_i of $\delta\underline{u}$, its contribution to the solution integrands in eq. (31) is

$$d[\delta\underline{x}(t,\tau)] = \underline{\tilde{\Phi}}_i \delta u_i d\tau. \tag{33}$$

Likewise, the individual covariance matrix element q_{ij} of Q has the contribution:

$$dP(t,\tau) = q_{ij}\left(\underline{\tilde{\Phi}}_i \underline{\tilde{\Phi}}_j^T\right) d\tau. \tag{34}$$

Hence, the influence vectors $\underline{\tilde{\Phi}}_i$ define the projection of each individual element of the input (measurement) error vector onto the entire output (state) error vector. Clearly, the columns of the input transition matrix constitute a basis for the time derivative of systematic error because the result for any error source must reside in the column space of $\tilde{\Phi}(t,\tau)$.

Similarly, the outer product influence matrices $\underline{\tilde{\Phi}}_i\underline{\tilde{\Phi}}_j^T$ are unity rank projection matrices defining the projection of each element of the input (measurement) covariance matrix onto the entire output (state) covariance matrix. Likewise, the complete set of influence matrices for all pairs (i, j) constitute a basis for the time derivative of random error covariance.

Equation (31) can now be rewritten in terms of influence matrices as

$$\delta\underline{x}(t) = \Phi(t,t_0)\delta\underline{x}(t_0) + \int_{t_0}^{t}\left(\sum_i \underline{\tilde{\Phi}}_i\delta u_i\right)d\tau$$

$$P(t) = \Phi(t,t_0)P(t_0)\Phi^T(t,t_0) + \int_{t_0}^{t}\left(\sum_i\sum_j q_{ij}\left(\underline{\tilde{\Phi}}_i\underline{\tilde{\Phi}}_j^T\right)\right)d\tau. \tag{35}$$

For later convenience, the following notation for influence matrices is defined:

$$\tilde{\Phi}_{ij} = \underline{\tilde{\Phi}}_i\underline{\tilde{\Phi}}_j^T. \tag{36}$$

The uppercase letter symbolizes a matrix, unlike the use of $\tilde{\phi}_{ij}$ which would be natural notation for a single element of the input transition matrix.

4.2.2. Error Moment Matrices

Note that the order of integration and summation can be reversed when convenient:

$$\delta\underline{x}(t) = \Phi(t,t_0)\delta\underline{x}(t_0) + \sum_i\left[\int_{t_0}^{t}\underline{\tilde{\Phi}}_i\delta u_i d\tau\right]$$

$$P(t) = \Phi(t,t_0)P(t_0)\Phi^T(t,t_0) + \sum_i\sum_j\left[\int_{t_0}^{t}q_{ij}\underline{\tilde{\Phi}}_i\underline{\tilde{\Phi}}_j^T d\tau\right]. \tag{37}$$

This is the error moment form of the error propagation equations. The two expressions in square brackets are the error moment vector and the error moment matrix, respectively. Both express how input errors are projected onto output errors by a convolution with the influence vector and matrix respectively.

For brevity, the following error moment matrix notation is defined:

$$\underline{u}_i = \int_{t_0}^{t}\left[\underline{\tilde{\Phi}}_i\delta u_i\right]d\tau \quad Q_{ij} = \int_{t_0}^{t}\left[q_{ij}\underline{\tilde{\Phi}}_i\underline{\tilde{\Phi}}_j^T\right]d\tau.$$

These moments represent the total contribution of a given individual error source onto the output error.

4.2.3. Trajectory Moment Matrices

When the errors are constant or can be rendered so under a change of variable, they can be moved outside the integrals to produce:

$$\delta\underline{x}(t) = \Phi(t,t_0)\delta\underline{x}(t_0) + \sum_i\left[\int_{t_0}^{t}\underline{\tilde{\Phi}}_i d\tau\right]\delta u_i$$

$$P(t) = \Phi(t,t_0)P(t_0)\Phi^T(t,t_0) + \sum_i\sum_j\left[\int_{t_0}^{t}\underline{\tilde{\Phi}}_i\underline{\tilde{\Phi}}_j^T d\tau\right]q_{ij}. \tag{38}$$

This is the trajectory moment form of the error propagation equations. The two expressions in square brackets are the trajectory moment vector and the trajectory moment matrix, respectively. Both are intrinsic properties of the trajectory, independent of the form of the errors.

For brevity, the following trajectory moment matrix notation is defined:

$$\underline{f}_i = \int_{t_0}^{t}\left[\underline{\tilde{\Phi}}_i\right]d\tau \quad F_{ij} = \int_{t_0}^{t}\left[\underline{\tilde{\Phi}}_i\underline{\tilde{\Phi}}_j^T\right]d\tau.$$

They usually take the form of collections of regular arrangements of all orders of scalar moments taken from the same family, where the family is spatial or Fourier as defined later.

4.3. Properties of Error Moment Matrices

Certain properties of the solution basis are evident at the matrix level. Error moment matrices are integrals of influence matrices which themselves are unity rank outer products. This section elicits some aspects of the behavior of such constructs.

4.3.1. Symmetry

Influence matrices occur in forms that are symmetric. Clearly:

$$\underline{\tilde{\Phi}}_i \underline{\tilde{\Phi}}_i^T = \text{ symmetric}$$

$$\underline{\tilde{\Phi}}_i \underline{\tilde{\Phi}}_j^T + \underline{\tilde{\Phi}}_j \underline{\tilde{\Phi}}_i^T = \underline{\tilde{\Phi}}_i \underline{\tilde{\Phi}}_j^T + \left(\underline{\tilde{\Phi}}_i \underline{\tilde{\Phi}}_j^T\right)^T = \text{ symmetric.}$$

The cross product matrices such as $\underline{\tilde{\Phi}}_i \underline{\tilde{\Phi}}_j^T$ will occur only in symmetric sums as shown; a consequence of their application to an input covariance which is symmetric.

4.3.2. Positive Semidefiniteness of Influence Matrices

Since covariance is positive semidefinite (represented notationally as $P, Q \geq 0$), it is to be expected that error moments and influence matrices will be positive semidefinite. It is easy to show that since $Q(\tau)$ is positive semidefinite, so is the quadratic form $\Phi(t, \tau)Q(\tau)\Phi(t, \tau)^T$ which represents the total time derivative of the state response.

Individual contributions may not be ≥ 0 however. Note that for an arbitrary vector $\underline{x}$:

$$\underline{x}^T \left(\underline{\tilde{\Phi}}_i \underline{\tilde{\Phi}}_i^T\right) \underline{x} = \left[\underline{x}^T \underline{\tilde{\Phi}}_i\right] \left[\underline{x}^T \underline{\tilde{\Phi}}_i\right]^T \geq 0$$

so the self outer product forms are ≥ 0. Little can be said about the cross product forms. The input projection matrix G may easily cause the sign of a diagonal element to be negative and positive semidefinite matrices cannot have negative numbers on their diagonals. Hence while the total derivative of state covariance is ≥ 0, it is the sum of several terms which themselves may not be.

4.3.3. Positive Semidefiniteness of Error Moment Matrices

At issue here is the behavior of the associated error moment matrix, the time integral of the influence matrix:

$$\boldsymbol{F}_{uu}(t) = \int_0^t \tilde{\Phi}_{uu}(t, \tau)d\tau. \tag{39}$$

In the case where $\frac{d}{dt}[\boldsymbol{F}_{uu}(t)] \geq 0$ then $\boldsymbol{F}_{uu}(t) \geq 0$ because for an arbitrary time-invariant vector $\underline{x}$:

$$\underline{x}^T \boldsymbol{F}_{uu}(t)\underline{x} = \int_0^t \underline{x}^T \left\{\frac{d}{dt}[\boldsymbol{F}_{uu}(\tau)]\right\} \underline{x}d\tau \geq 0. \tag{40}$$

The integrand is a non-negative scalar by assumption. Therefore, $\underline{x}^T \boldsymbol{F}_{uu}(t)\underline{x} \geq 0$; the defining property of positive semidefiniteness applies to $\boldsymbol{F}_{uu}(t)$.

It follows that $\boldsymbol{F}_{uu}(t)$ has all of these properties:

- all eigenvalues are non-negative;

- all diagonal elements are non-negative

- the determinants of all of its leading principle minors are nonnegative. These are all the square submatrices which contain the top left element.

4.3.4. Monotonicity

A more interesting question is: if the derivative is ≥ 0, is the state covariance monotone in any sense? That is, does random error always increase in odometry in some sense?

When $\frac{d}{dt}[\boldsymbol{F}_{uu}(t)] \geq 0$, by definition:

$$\underline{x}^T \left\{\frac{d}{dt}[\boldsymbol{F}_{uu}(t)]\right\} \underline{x} = \frac{d}{dt}\left[\underline{x}^T \boldsymbol{F}_{uu}(t)\underline{x}\right] \geq 0.$$

Consider the case where the arbitrary vector $\underline{x}$ above is an (normalized) eigenvector of $\boldsymbol{F}_{uu}(t)$. Then, this becomes:

$$\frac{d}{dt}[\lambda_i] \geq 0. \tag{41}$$

Hence, when the time derivative matrix is positive semidefinite, every eigenvalue of $\boldsymbol{F}_{uu}(t)$ is non-decreasing. Therefore, also its trace, its determinant, its norm, and indeed its "magnitude" in any direction $\underline{x}$ defined by the Rayleigh quotient:

$$mag(\boldsymbol{F}_{uu}(t)) = \frac{\|\underline{x}^T \boldsymbol{F}_{uu}(t)\underline{x}\|}{\|\underline{x}^T \underline{x}\|}$$

are all non-decreasing functions of time. So $\boldsymbol{F}_{uu}(t)$ is non-decreasing in virtually every reasonable and practical sense. In a movie showing error ellipses of this matrix in principle coordinates, the entire ellipse at any point in time will always be contained entirely outside the ellipse just slightly earlier in time.

4.3.5. Positive Semidefiniteness of the Error Moment Time Derivative

The question to be addressed next is when is $\frac{d}{dt}[\boldsymbol{F}_{uu}(t)] \geq 0$. Using the Leibnitz rule:

$$\frac{d}{dt}[\boldsymbol{F}_{uu}(t)] = \int_0^t \left[\frac{\partial}{\partial t}\tilde{\Phi}_{uu}(t, \tau)\right] d\tau + \tilde{\Phi}_{uu}(t, t). \tag{42}$$

When the influence matrix does not depend on the limits of integration, $\Phi_{uu}(t, \tau) = \Phi_{uu}(\tau)$, the first term vanishes and the derivative is ≥ 0. However, in the general case, the issue rests on the character of $\frac{\partial}{\partial t}\Phi_{uu}(t, \tau)$ because $\Phi_{uu} \geq 0$. If this partial derivative matrix is positive semidefinite, so is the time derivative.

4.3.6. Conservation

A useful scalar representing the size of a covariance matrix is the so-called "total variance" given by the covariance matrix trace. Taking the trace of eq. (42) and interchanging the order of operations:

$$\frac{d}{dt}\left[tr\left(\boldsymbol{F}_{uu}(t)\right)\right] = \int_0^t tr\left[\frac{\partial}{\partial t}\tilde{\Phi}_{uu}(t, \tau)\right]d\tau \tag{43}$$
$$+ \left[tr\left(\tilde{\Phi}_{uu}(t, t)\right)\right].$$

Now the trace of the partial derivative matrix determines when the time derivative of total variance is non-negative (a less stringent condition than positive definiteness).

By definition:

$$tr\left(\boldsymbol{F}_{uu}(t)\right) = \int_0^t \frac{d}{dt}\left[tr\left(\boldsymbol{F}_{uu}(\tau)\right)\right]d\tau. \tag{44}$$

When the time derivative of total variance is non-negative, the total variance itself is monotone.

Again, when the influence matrix does not depend on the limits of integration, $tr(\Phi_{uu}(t, t)) \geq 0$ which guarantees monotonicity.

In either case, even when total variance is monotone, indeed even when every eigenvalue is monotone, there is no guarantee that individual diagonal elements cannot decrease. What can be said is that any decrease in one diagonal element must be offset by at least as great an increase in the rest in order for the sum to be conserved or increased. Intuitively, even monotone uncertainty ellipses may rotate in space causing momentary decreases in diagonal elements.

5. Scalar Moments of Error

It is useful to focus at times on the individual scalar elements of the error moment matrices, called simply error moments. Relatively few scalar functionals recur often and repopulate the error moment matrices under various different circumstances. These scalar functionals evaluated on trajectories encode the path dependent nature of error in odometry.

5.1. Error Moments

Individual elements of the solution integrals of the last section can be interpreted as line integrals in state space, evaluated over the reference trajectory, where the integrand is some projection of input error onto the relevant differentials of the state space error trajectory. Line integrals may already be present and when they are not, they can often be generated by substituting error models. Consider a term of the form:

$$\delta x(t) = \int_0^t f\left[x(\tau)\right]\delta V(\tau)d\tau.$$

If the input error is motion-dependent, which is to say proportional to a power of velocity (or some other position variable derivative):

$$\delta V(\tau) = \alpha(\tau)V^n(\tau)$$

then the integral becomes

$$\delta x(s) = \int_0^s f\left[x(s)\right]\alpha(s)V^{n-1}(s)ds$$

which is a line integral where s is arc length (or some other position variable) along the trajectory.

Such path functionals are equivalent to the moments of mechanics evaluated on curves where the "mass" at a given location is the error magnitude suffered at that location. They can also be considered to be moments of error evaluated over a curve in state space. Many moments that appear in odometry problems take the form:

$$E(t) = \int_0^t \Delta x^a(t, \tau)\Delta y^b(t, \tau)\cos\theta(\tau)^c \tag{45}$$
$$\sin\theta(\tau)^d\varepsilon(\tau)d\tau$$

where a, b, c, and d are non-negative integers ≤ 2. For convenience, the order of the moment is defined as the sum of all of these exponents. In most cases, first-order moments determine systematic error propagation whereas second-order ones determine stochastic error propagation. The error models $\varepsilon(\tau)$ consist respectively of either the deterministic error $\delta u_i(\tau)$ or the second-order statistics $\sigma_{ij}(\tau)$ of a random error probability distribution. The resulting moment $E(t)$ will correspond to a systematic error in pose, the mean of a random error, or a variance or covariance.

The following shorthand expressions for the coordinates of the endpoint from the perspective of the point $[x(\tau), y(\tau)]$ are defined:

$$\Delta x(t, \tau) = [x(t) - x(\tau)]$$
$$\Delta y(t, \tau) = [y(t) - y(\tau)]. \tag{46}$$

5.2. Trajectory Moments

When errors have particularly simple forms, they can be moved outside the integral signs in the solution equations

by changes of variable which render them constant. Under these conditions, the associated component of the solution integral, the trajectory moment, becomes dependent solely on the geometry of the trajectory followed.

5.2.1. Duration, Excursion, and Rotation Moments

Moments can be distinguished based on the essential variable of integration. When the error model is proportional to time (such as in a gyro):

$$\varepsilon(\tau)d\tau = k \times d\tau.$$

Ignoring the constant factor, the associated moment will be called a duration moment and takes the form:

$$T(t) = \int_0^t \Delta x^a(t, \tau) \Delta y^b(t, \tau)$$

$$\cos\theta(\tau)^c \sin\theta(\tau)^d d\tau. \tag{47}$$

When the error model is proportional to linear velocity (as in an encoder) $d\xi/d\tau$:

$$\varepsilon(\tau)d\tau = k \times (d\xi/d\tau) \times d\tau = k \times d\xi.$$

Ignoring the constant factor, the associated moment will be called an excursion moment and takes the form:

$$S(s) = \int_0^s \Delta x^a(s, \xi) \Delta y^b(s, \xi) \cos\theta(\xi)^c \sin\theta(\xi)^d d\xi. \tag{48}$$

When the error model is proportional to angular velocity $d\zeta/d\tau$:

$$\varepsilon(\tau)d\tau = k \times (d\zeta/d\tau) \times d\tau = k \times d\zeta.$$

Ignoring the constant factor, the associated moment will be called a rotation moment and takes the form:

$$\Theta(\theta) = \int_0^\theta \Delta x^a(\theta, \zeta) \Delta y^b(\theta, \zeta) \cos\zeta^c \sin\zeta^d d\zeta. \tag{49}$$

5.2.2. Spatial, Fourier, and Hybrid Moments

Moments can also be distinguished based on the form of the integrand. When $c = d = 0$ the moment is a spatial moment. The spatial moments are equivalent to the moment of inertia of curves, the moments of arc, and apply to angular velocity errors. Likewise, the total variance is the analog of the polar moment of inertia. The first spatial trajectory moments are:

$$T_x(t) = \int_0^t [x(t) - x(\tau)]\, d\tau$$

$$S_x(s) = \int_0^s [x(s) - x(\zeta)]\, d\zeta \tag{50}$$

$$\Theta_x(\theta) = \int_0^\theta [x(\theta) - x(\xi)]\, d\xi.$$

In order, these will be called the first spatial duration, first spatial excursion, and first spatial rotation moments. Equivalent moments for the y coordinate and for higher orders are immediate.

When $a = b = 0$ the moment will be called a Fourier moment because it is related to the Fourier sine and cosine transforms. The Fourier moments apply to linear velocity errors. The first Fourier trajectory moments are:

$$T_c(t) = \int_0^t \cos\theta(\tau) d\tau$$

$$S_c(s) = \int_0^s \cos\theta(\zeta) d\zeta \tag{51}$$

$$\Theta_c(\theta) = \int_0^\theta \cos\theta(\xi) d\xi.$$

In order, these will be called the first Fourier cosine duration, first Fourier cosine excursion, and first Fourier cosine rotation moments. Equivalent moments for the sine function and higher orders are immediate.

Moments that are not purely spatial or Fourier moments (for example, when $b = d = 0$) will be called hybrid moments. These are responsible for the propagation of certain correlated errors.

5.2.3. Moment Notation

Moments will be denoted in a manner similar to covariance and the moments of inertia where repeated subscripts identify the exponents and overall order of the moment. For second-order moments, the principal moments are those whose subscripts are equal and the cross moments are all the rest. For example, a spatial, second-order, principal, excursion moment and a hybrid, second-order, cross, duration trajectory moment are

$$S_{yy} = \int\limits_0^s [y(s) - y(\xi)]^2 \, d\xi$$

$$(52)$$

$$T_{xc} = \int\limits_0^t [x(t) - x(\tau)] \cos\theta(\tau) d\tau.$$

5.2.4. Recursive Evaluation

The spatial moments can be difficult to evaluate numerically due to the dependence of the integrand on the variable of integration. However, an expansion of the integrand generates a set of component integrals which can be evaluated recursively. For example:

$$T_{yy}(t) = ty^2(t) - 2y(t) \int\limits_0^t y(\tau)d\tau + \int\limits_0^t y^2(\tau)d\tau. \quad (53)$$

This is essentially the derivation of the parallel axis theorem of inertia. The two remaining integrals are the first and second moments of arc along the trajectory.

For the second Fourier moments, note that

$$\Theta_{cc}(\theta) = \int\limits_0^\theta [\cos\theta(\xi)]^2 \, d\xi = \frac{\theta}{2} + \int\limits_0^\theta [\cos 2\theta(\xi)] \, d\xi.$$

So the first and second Fourier moments are determined by the first and second coefficients in the Fourier series.

5.3. Properties of Trajectory Moments

Trajectory moments are responsible for many of the interesting behaviors of error propagation. A few of the most important are discussed here.

5.3.1. Path Independence

Certain moments are path-independent. For example, the first-order Fourier excursion moments are just the coordinates of the endpoints:

$$S_c = \int\limits_0^s \cos\theta ds = x(s) \quad (54)$$

so they must vanish on closed trajectories. As a result, it can be shown that scale errors in measurements of distance traveled or velocity are not observable on closed trajectories because they always vanish.

5.3.2. Motion Dependence

Excursion and rotation moments are motion-dependent by definition because time has been eliminated as the variable of integration and replaced by distance or angle.

5.3.3. Reversibility

While time advances monotonically, the differentials ds and $d\theta$ get their signs from the signs of the associated linear and angular velocities because

$$ds = Vdt \quad d\theta = \omega dt.$$

All motion-dependent (excursion and rotation) moments are reversible in the independent variable because

$$\int\limits_0^s F\left[\underline{u}(s)\right] ds = -\int\limits_s^0 F(\underline{u}(s)) ds. \quad (55)$$

A more important question is whether it is practically possible for the integrand to remain unchanged when the direction of integration is reversed. If the integrand is an even function of the inputs, then reversing the inputs (by switching the order of the limits of integration) will change the sign of ds but not that of the integrand and the system will be reversible. For odometry, it is important that any of these equivalent conditions be met:

- the integrand is an even function of velocity;

- the original system differential equation for $d\underline{x}/dt$ is odd in velocity;

- the original distance differential equation for $d\underline{x}/ds$ is even in velocity.

5.3.4. Irreversibility

While certain motion-dependent systematic errors (first-order moments) are reversible, random errors (second-order moments) generally are not. In the case of second-order moments, it is usually appropriate to interpret the differentials ds and $d\theta$ as unsigned quantities (unless the context is one of running time backwards) in order to ensure that the associated variance increases in both directions of motion. For principal second-order moments, the integrand itself is always positive. In these cases, this irreversibility of the input variances can be accomplished as follows:

$$ds = |V|dt \quad d\theta = |\omega|dt.$$

5.3.5. Symmetry, Centroids, and Zeros

First-order moments and second-order cross moments may vanish at specific places whether or not the trajectory closes there. For example, the first spatial moments can be written in terms of the current position, the distance traveled and the instantaneous centroid location:

$$S_x = sx(s) - \int\limits_0^s x(\xi)d\xi = s[x(s) - \bar{x}(s)]. \quad (56)$$

Hence, all first spatial excursion moments vanish at the centroid of the associated coordinate. This observation subsumes earlier comments on symmetry as a special case.

5.3.6. Interrelationships

Derivatives (integrals) of trajectory moments are often equal to lower-order (higher-order) moments. For example, Leibnitz rule when the integrand depends on the limits of integration is:

$$\frac{d}{ds} \int_0^s f(s, \xi) d\xi = \int_0^s \frac{\partial}{\partial s} f(s, \xi) d\xi + f(s, s). \quad (57)$$

Applying this to a second-order spatial moment yields:

$$\frac{dS_{xx}}{ds} = \frac{d}{ds} \left\{ \int_0^s [x(s) - x(\xi)]^2 \, d\xi \right\}$$

$$\frac{dS_{xx}}{ds} = \int_0^s 2 [x(s) - x(\xi)] x'(s) d\xi = 2 \cos \theta \, S_x(s). \quad (58)$$

Thus, systematic and random error propagation are inextricably related. Indeed, zeros of the first-order moments can coincide with extrema of the second-order moments, etc.

5.3.7. Monotonicity

The previous example also illustrates the case where a second-order moment, despite its squared integrand, is not monotone. As mentioned earlier, the cause can be traced to the dependence of the integrand on the integration limits.

In practical terms, the spatial moments such as S_{xx} are associated with angular velocity indications. In this case, even the total position variance of the associated error moment matrix is not necessarily monotone.

On the other hand, the integrands of the Fourier moments do not depend on the limits. Thus:

$$\frac{d}{ds}(S_{cc}) = \frac{d}{ds} \left(\int_0^s [\cos \theta^2] ds \right) = \cos \theta^2 \geq 0$$

is monotone on any trajectory.

5.3.8. Conservation

The composite behavior of the gradient of the total translational variance for the Fourier moments is

$$\frac{d}{ds}(S_{cc} + S_{ss}) = \frac{d}{ds} \left(\int_0^s [\cos \theta^2 + \sin^2 \theta] ds \right) = 1.$$

In the event that any one diagonal term momentarily stops increasing, the other term compensates by increasing more rapidly such that the total variance grows monotonically with distance at a fixed rate regardless of the shape of the trajectory.

On a trajectory for which curvature is constant, for example, this interplay is the second harmonic rotation of a monotonically growing uncertainty ellipse.

6. Transition Matrix of Time-Varying Systems

Given that the system Jacobian of odometry is a time-varying matrix, linear systems theory shows that the transition matrix exists, but generally provides little guidance in finding it. Luckily, odometry is a special case.

6.1. Transition Matrix

Consider the following particular matrix exponential of a definite integral of the system Jacobian:

$$\Psi(t, \tau) = \exp \left(\int_\tau^t F(\zeta) d\zeta \right) = \exp[R(t, \tau)] \quad (59)$$

where the matrix exponential is defined as usual by the infinite matrix power series:

$$\exp(A) = I + A + \frac{A^2}{2!} + \frac{A^3}{3!} + \dots .$$

When this commutes (Brogan 1974) with the system dynamics matrix:

$$\Psi(t, \tau) F(t) = F(t) \Psi(t, \tau) \quad (60)$$

then every power of $R(t, \tau)$ also commutes with $F(t)$ and the derivative is

$$\frac{d}{dt} \Psi(t, \tau) = \frac{d}{dt} \left\{ I + R(t, \tau) + \frac{R(t, \tau)^2}{2!} \right.$$

$$\left. + \frac{R(t, \tau)^3}{3!} + \dots \right\} \quad (61)$$

$$= F(t) \Psi(t, \tau).$$

Thus, it satisfies eq. (30) and therefore it is the transition matrix which solves the associated time-varying linear system. This property of commutative dynamics is the key to generating a general solution to the error propagation equations of odometry. Once a closed-form expression for the transition matrix is available, everything else follows from classical theory.

6.1.1. Strict Upper Triangularity

The echelon form common in odometry means that the system Jacobian $F(t)$ is strictly upper triangular:

$$F = \{f_{ij} | f_{ij} = 0 \text{ when } (j \leq i)\} \qquad (62)$$

and since $\Psi(t, \tau)$ is composed entirely of definite integrals of $F(t)$, it is also strictly upper triangular. It can be shown that the nth power (and hence all subsequent powers) of an $n \times n$ strictly upper triangular matrix vanishes. This means that the matrix exponential can be easily written by summing the first few non-zero terms. This property means that closed-form expressions for the transition matrix are available because the exponential series can be no longer than n terms.

6.2. Commutative Dynamics

It is easy to see that if

$$R(t, \tau)F(t) = F(t)R(t, \tau) \qquad (63)$$

then eq. (60) is also satisfied (the converse was argued earlier). Generally speaking, this means that the system Jacobian must commute with its own definite integral ("commutative dynamics"). If both matrices share a complete set of distinct eigenvectors, commutability is guaranteed, but odometry is a different case.

6.3. Strict Upper Rectangularity

In fact, two-dimensional (2D) odometry has a slightly more special structure than simple echelon form. The dynamic equations (and system Jacobian) have the property that if one state variable depends on another, the second does not depend on a third. Pictorially, the system Jacobian has the structure shown in Figure 3.

Here, this property will be called strict upper rectangularity

$$F = \{f_{ij} | f_{ij} = 0 \text{ when } (j \leq k \text{ or } i \leq n - k - 1)\}. \qquad (64)$$

Such a matrix is singular and indeed highly rank deficient and its row and column spaces are orthogonal. The limit of unity for state variable dependences implies that $F^2(t) = 0$. The definition of $R(t, \tau)$ (a definite integral of $F(t)$) implies that it has the same structure. Therefore:

$$R^2(t, \tau) = F(t)R(t, \tau) = R(t, \tau)F(t) = 0. \qquad (65)$$

Such a system clearly satisfies eq. (63) and hence eq. (60). Additionally, the series for the matrix exponential truncates after just one term

$$\Psi(t, \tau) = \exp[R(t, \tau)] = I + R(t, \tau)$$

and eq. (60) takes the form:

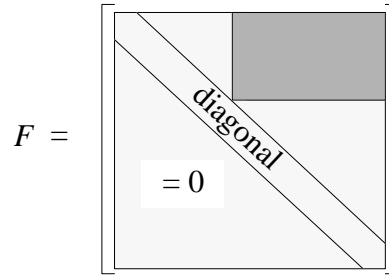$$\Psi(t, \tau)F(t) = F(t)\Psi(t, \tau) = F(t). \qquad (66)$$

$$F =$$

diagonal

$$= 0$$

Fig. 3. Strict upper rectangularity; state variable dependences are no more than one deep.

6.4. Derivation by Partial Differentiation

A second method of deriving the transition matrix is also important for the case of three-dimensional (3D) odometry. By definition in the case of perturbative dynamics:

$$\delta \underline{x}(t) = \Phi(t, \tau)\delta \underline{x}(\tau). \qquad (67)$$

The dynamics are, by definition, linear. Hence any device which generates a linear relationship between $\delta \underline{x}(t)$ and $\delta \underline{x}(\tau)$ will generate the transition matrix. Consider the Jacobian matrix relating these two:

$$d\underline{x}(t) = \left[\frac{\partial \underline{x}(t)}{\partial \underline{x}(\tau)}\right] d\underline{x}(\tau). \qquad (68)$$

Normally a Jacobian is used to approximate a nonlinear system locally; however, because the system is linear, the Jacobian is the transition matrix in this case. One way to obtain this Jacobian is to find a nonlinear relationship between $\underline{x}(t)$ and $\underline{x}(\tau)$ and take its Jacobian. Such relationships can often be derived for odometry based on 2D and 3D kinematics.

7. Application To Odometry

This section will derive the error propagation equations for a few common forms of odometry. Without loss of generality, let the system start at time $t_0 = 0$. Distance traveled will be denoted by s.

7.1. Direct Heading Odometry

The term direct heading odometry will be used to refer to the case where a direct measurement of heading is available rather than its derivative. For example, a compass could be used to measure heading directly and a transmission encoder could be used to measure the linear velocity of the center of an axle of the vehicle.

The heading and error in heading are respectively equal at all times to the heading measurement and its error. Therefore, considering the heading to be an input, the state equations are:

$$\frac{d}{dt}\begin{bmatrix} x(t) \\ y(t) \end{bmatrix} = \begin{bmatrix} V(t)\cos\theta(t) \\ V(t)\sin\theta(t) \end{bmatrix} \qquad (69)$$

where

$$\underline{x}(t) = \begin{bmatrix} x(t) & y(t) \end{bmatrix}^T$$

$$\underline{u}(t) = \begin{bmatrix} V(t) & \theta(t) \end{bmatrix}^T$$

$$\delta\underline{x}(t) = \begin{bmatrix} \delta x(t) & \delta y(t) \end{bmatrix}^T \tag{70}$$

$$\delta\underline{u}(t) = \begin{bmatrix} \delta V(t) & \delta\theta(t) \end{bmatrix}^T$$

$$P(t) = \begin{bmatrix} \sigma_{xx} & \sigma_{xy} \\ \sigma_{xy} & \sigma_{yy} \end{bmatrix} \quad Q(t) = \begin{bmatrix} \sigma_{vv} & \sigma_{v\theta} \\ \sigma_{v\theta} & \sigma_{\theta\theta} \end{bmatrix}.$$

This system is homogeneous with respect to the velocity input but not with respect to the heading input. The Jacobians are:

$$F(t) = \begin{bmatrix} 0 & 0 \\ 0 & 0 \end{bmatrix} G(t) = \begin{bmatrix} c\theta(t) & -V(t)s\theta(t) \\ s\theta(t) & V(t)c\theta(t) \end{bmatrix}. \tag{71}$$

So the linearized error dynamics are:

$$\frac{d}{dt}\begin{bmatrix} \delta x(t) \\ \delta y(t) \end{bmatrix} = \begin{bmatrix} 0 & 0 \\ 0 & 0 \end{bmatrix}\begin{bmatrix} \delta x(t) \\ \delta y(t) \end{bmatrix} + \begin{bmatrix} c\theta & -Vs\theta \\ s\theta & Vc\theta \end{bmatrix}\begin{bmatrix} \delta V(t) \\ \delta\theta(t) \end{bmatrix}. \tag{72}$$

In this general form, the error dynamics are not homogeneous with respect to the velocity input.

7.1.1. Transition Matrix

Noting that the Jacobian satisfies eq. (63) trivially, the rest of the operations and matrices leading to the input transition matrix are as follows:

$$R(t, \tau) = \int_\tau^t F(\zeta)d\zeta = \int_\tau^t \begin{bmatrix} 0 & 0 \\ 0 & 0 \end{bmatrix} d\zeta = \begin{bmatrix} 0 & 0 \\ 0 & 0 \end{bmatrix}$$

$$\Phi(t, \tau) = \Psi(t, \tau) = \exp[R(t, \tau)] = \begin{bmatrix} 1 & 0 \\ 0 & 1 \end{bmatrix}$$

$$\tilde{\Phi}(t, \tau) = \Phi(t, \tau)G(\tau) = \begin{bmatrix} c\theta(\tau) & -V(\tau)s\theta(\tau) \\ s\theta(\tau) & V(\tau)c\theta(\tau) \end{bmatrix}. \tag{73}$$

Note that $V(t)c\theta(t) = \dot{x}(t)$, etc., could be substituted here.

7.1.2. Solution in Matrix Form

Substituting into the general solution in eq. (31) gives

$$\delta\underline{x}(t) = \delta\underline{x}(0) + \int_0^t \begin{bmatrix} c\theta & -Vs\theta \\ s\theta & Vc\theta \end{bmatrix}\begin{bmatrix} \delta V(t) \\ \delta\theta(t) \end{bmatrix}d\tau \tag{74}$$

$$P(t) = P(0) + \int_{t_0}^t \begin{bmatrix} c\theta & -Vs\theta \\ s\theta & Vc\theta \end{bmatrix}\begin{bmatrix} \sigma_{vv} & \sigma_{v\theta} \\ \sigma_{v\theta} & \sigma_{\theta\theta} \end{bmatrix}$$

$$\begin{bmatrix} c\theta & -Vs\theta \\ s\theta & Vc\theta \end{bmatrix}^T d\tau.$$

This result is the general linearized solution for the propagation of systematic and random error in 2D direct heading odometry for any trajectory and any error model. When the velocity error is a scale error (i.e., $\delta V(t) \propto V(t)$), its effects are path-independent.

7.1.3. Solution in Error Moment Form

The error moment form of the solution is

$$\delta\underline{x}(t) = \delta\underline{x}(0) + \int_0^t \underline{\tilde{\Phi}}_v(\tau)\delta V d\tau + \int_0^t \underline{\tilde{\Phi}}_\theta(\tau)\delta\theta d\tau$$

$$P(t) = P(0) + \int_0^t \tilde{\Phi}_{vv}(\tau)\sigma_{vv}d\tau \tag{75}$$

$$+ \int_0^t \left(\tilde{\Phi}_{v\theta}(\tau) + \tilde{\Phi}_{\theta v}(\tau) \right)\sigma_{v\theta}d\tau + \int_0^t \tilde{\Phi}_{\theta\theta}(\tau)\sigma_{\theta\theta}d\tau.$$

The relevant influence matrices are

$$\underline{\tilde{\Phi}}_v(\tau) = \begin{bmatrix} c\theta & s\theta \end{bmatrix}^T \quad \underline{\tilde{\Phi}}_\theta(\tau) = \begin{bmatrix} -Vs\theta & Vc\theta \end{bmatrix}^T$$

$$\tilde{\Phi}_{vv}(\tau) = \begin{bmatrix} c\theta \\ s\theta \end{bmatrix}\begin{bmatrix} c\theta \\ s\theta \end{bmatrix}^T = \begin{bmatrix} c^2\theta & c\theta s\theta \\ c\theta s\theta & s^2\theta \end{bmatrix}$$

$$\tilde{\Phi}_{v\theta}(\tau) = \tilde{\Phi}_{\theta v}^T(\tau) = \begin{bmatrix} c\theta \\ s\theta \end{bmatrix}\begin{bmatrix} -Vs\theta \\ Vc\theta \end{bmatrix}^T = V\begin{bmatrix} -c\theta s\theta & c^2\theta \\ s^2\theta & c\theta s\theta \end{bmatrix}$$

$$\tilde{\Phi}_{\theta\theta}(\tau) = \begin{bmatrix} -Vs\theta \\ Vc\theta \end{bmatrix}\begin{bmatrix} -Vs\theta \\ Vc\theta \end{bmatrix}^T = V^2\begin{bmatrix} s^2\theta & -c\theta s\theta \\ -c\theta s\theta & c^2\theta \end{bmatrix}. \tag{76}$$

These appear in the error moment form of the general solution:

$$\delta\underline{x}(t) = \delta\underline{x}(0) + \int_0^t \begin{bmatrix} c\theta \\ s\theta \end{bmatrix}\delta V d\tau + \int_0^t V\begin{bmatrix} -s\theta \\ c\theta \end{bmatrix}\delta\theta d\tau$$

$$P(t) = P(0) + \int_0^t \begin{bmatrix} c^2\theta & c\theta s\theta \\ c\theta s\theta & s^2\theta \end{bmatrix}\sigma_{vv}d\tau \tag{77}$$

$$+ \int_0^t \begin{bmatrix} -2c\theta s\theta & 1 \\ 1 & 2c\theta s\theta \end{bmatrix}V\sigma_{v\theta}d\tau$$

$$+ \int_0^t \begin{bmatrix} s^2\theta & -c\theta s\theta \\ -c\theta s\theta & c^2\theta \end{bmatrix}V^2\sigma_{\theta\theta}d\tau.$$

Note that $V c\theta d\tau = dx$, etc., could be substituted here to convert the second integral in the first equation to a line integral.

7.2. Integrated Heading Odometry

In integrated heading odometry, an angular velocity indication is available and a heading state is determined by integrating it. For example, a gyro could be used to measure heading rate and a transmission encoder, groundspeed radar, or fifth wheel encoder could be used to measure the linear velocity of the center of an axle of the vehicle. This is the case given in eq. (2) repeated here for reference:

$$\frac{d}{dt}\begin{bmatrix} x(t) \\ y(t) \\ \theta(t) \end{bmatrix} = \begin{bmatrix} V(t)\cos\theta(t) \\ V(t)\sin\theta(t) \\ \omega(t) \end{bmatrix} \tag{78}$$

where

$$\underline{x}(t) = \begin{bmatrix} x(t) & y(t) & \theta(t) \end{bmatrix}^T$$
$$\underline{u}(t) = \begin{bmatrix} V(t) & \omega(t) \end{bmatrix}^T \tag{79}$$

$$\delta\underline{x}(t) = \begin{bmatrix} \delta x(t) & \delta y(t) & \delta\theta(t) \end{bmatrix}^T$$

$$\delta\underline{u}(t) = \begin{bmatrix} \delta V(t) & \delta\omega(t) \end{bmatrix}^T$$

$$P(t) = \begin{bmatrix} \sigma_{xx} & \sigma_{xy} & \sigma_{x\theta} \\ \sigma_{xy} & \sigma_{yy} & \sigma_{y\theta} \\ \sigma_{x\theta} & \sigma_{y\theta} & \sigma_{\theta\theta} \end{bmatrix} \quad Q(t) = \begin{bmatrix} \sigma_{vv} & \sigma_{v\omega} \\ \sigma_{v\omega} & \sigma_{\omega\omega} \end{bmatrix}.$$

If $\kappa(t)$ is the trajectory curvature, then

$$\omega(t) = \kappa(t)V(t).$$

Under this substitution it is clear that this system is homogeneous to the first degree in the input velocity. The Jacobians are

$$F(t) = \begin{bmatrix} 0 & 0 & -Vs\theta \\ 0 & 0 & Vc\theta \\ 0 & 0 & 0 \end{bmatrix} \quad G(t) = \begin{bmatrix} c\theta(t) & 0 \\ s\theta(t) & 0 \\ 0 & 1 \end{bmatrix}. \tag{80}$$

So the linearized error dynamics are

$$\frac{d}{dt}\begin{bmatrix} \delta x(t) \\ \delta y(t) \\ \delta\theta(t) \end{bmatrix} = \begin{bmatrix} 0 & 0 & -Vs\theta \\ 0 & 0 & Vc\theta \\ 0 & 0 & 0 \end{bmatrix}\begin{bmatrix} \delta x(t) \\ \delta y(t) \\ \delta\theta(t) \end{bmatrix}$$
$$+ \begin{bmatrix} c\theta(t) & 0 \\ s\theta(t) & 0 \\ 0 & 1 \end{bmatrix}\begin{bmatrix} \delta V(t) \\ \delta\omega(t) \end{bmatrix}. \tag{81}$$

In this general form, the system is not homogeneous with respect to the input velocity.

7.2.1. Transition Matrix

Noting the upper rectangular Jacobian, the rest of the operations and matrices leading to the input transition matrix are as follows:

$$R(t,\tau) = \int_\tau^t \begin{bmatrix} 0 & 0 & -Vs\theta \\ 0 & 0 & Vc\theta \\ 0 & 0 & 0 \end{bmatrix} d\zeta = \begin{bmatrix} 0 & 0 & -\Delta y(t,\tau) \\ 0 & 0 & \Delta x(t,\tau) \\ 0 & 0 & 0 \end{bmatrix}$$

$$\Psi(t,\tau) = \exp[R(t,\tau)] = I + R = \begin{bmatrix} 1 & 0 & -\Delta y(t,\tau) \\ 0 & 1 & \Delta x(t,\tau) \\ 0 & 0 & 1 \end{bmatrix}$$

$$\tilde{\Phi}(t,\tau) = \Phi(t,\tau)G(\tau) = \begin{bmatrix} c\theta(\tau) & -\Delta y(t,\tau) \\ s\theta(\tau) & \Delta x(t,\tau) \\ 0 & 1 \end{bmatrix}. \tag{82}$$

The matrix exponential follows from the fact that $R^2(t,\tau) = 0$ in this case. The expressions $\Delta x(t,\tau)$ and $\Delta y(t,\tau)$ are defined in eq. (46). Integrals involving these quantities in particular must be manipulated with slightly more care to preserve the distinction between t (the endpoint of the trajectory) and τ (the variable of integration).

7.2.2. Solution in Matrix Form

Substituting into the general solution in eq. (31) gives

$$\delta\underline{x}(t) = \underline{IC_d} + \int_0^t \begin{bmatrix} c\theta & -\Delta y(t,\tau) \\ s\theta & \Delta x(t,\tau) \\ 0 & 1 \end{bmatrix}\begin{bmatrix} \delta V(\tau) \\ \delta\omega(\tau) \end{bmatrix} d\tau$$

$$P(t) = IC_s + \int_0^t \begin{bmatrix} c\theta & -\Delta y(t,\tau) \\ s\theta & \Delta x(t,\tau) \\ 0 & 1 \end{bmatrix}\begin{bmatrix} \sigma_{vv} & \sigma_{v\omega} \\ \sigma_{v\omega} & \sigma_{\omega\omega} \end{bmatrix} \tag{83}$$
$$\begin{bmatrix} c\theta & -\Delta y(t,\tau) \\ s\theta & \Delta x(t,\tau) \\ 0 & 1 \end{bmatrix}^T d\tau$$

where the initial state response for this case is

$$\underline{IC_d} = \begin{bmatrix} 1 & 0 & -y(t) \\ 0 & 1 & x(t) \\ 0 & 0 & 1 \end{bmatrix}\delta\underline{x}(0) = \begin{bmatrix} \delta x(0) \\ \delta y(0) \\ 0 \end{bmatrix}$$

$$+ \begin{bmatrix} -y(t)\delta\theta(0) \\ x(t)\delta\theta(0) \\ \delta\theta(0) \end{bmatrix}$$

$$IC_s = \begin{bmatrix} 1 & 0 & -y(t) \\ 0 & 1 & x(t) \\ 0 & 0 & 1 \end{bmatrix}\begin{bmatrix} \sigma_{xx}(0) & \sigma_{xy}(0) & \sigma_{x\theta}(0) \\ \sigma_{xy}(0) & \sigma_{yy}(0) & \sigma_{y\theta}(0) \\ \sigma_{x\theta}(0) & \sigma_{y\theta}(0) & \sigma_{\theta\theta}(0) \end{bmatrix} \tag{84}$$

$$\begin{bmatrix} 1 & 0 & -y(t) \\ 0 & 1 & x(t) \\ 0 & 0 & 1 \end{bmatrix}^T.$$

This result is the general linearized solution for the propagation of systematic and random error in 2D integrated heading odometry for any trajectory and any error model.

7.2.3. Solution in Error Moment Form

The error moment form of the solution is

$$\delta \underline{x}(t) = \underline{IC}_d + \int_{t_0}^{t} \underline{\tilde{\Phi}}_v(\tau) \delta V d\tau + \int_0^t \underline{\tilde{\Phi}}_\omega(\tau) \delta \omega d\tau$$

$$P(t) = IC_s + \int_0^t \left[\tilde{\Phi}_{v\omega}(\tau) + \tilde{\Phi}_{\omega v}(\tau) \right] \sigma_{v\omega} d\tau \qquad (85)$$

$$+ \int_0^t \tilde{\Phi}_{vv}(\tau) d\tau + \int_0^t \tilde{\Phi}_{\omega\omega}(\tau) \sigma_{\omega\omega} d\tau.$$

The relevant influence matrices are

$$\underline{\tilde{\Phi}}_v(\tau) = \begin{bmatrix} c\theta & s\theta & 0 \end{bmatrix}^T$$

$$\underline{\tilde{\Phi}}_\omega(\tau) = \begin{bmatrix} -\Delta y(t,\tau) & \Delta x(t,\tau) & 1 \end{bmatrix}^T$$

$$\tilde{\Phi}_{vv}(\tau) = \begin{bmatrix} c\theta \\ s\theta \\ 0 \end{bmatrix} \begin{bmatrix} c\theta \\ s\theta \\ 0 \end{bmatrix}^T = \begin{bmatrix} c^2\theta & c\theta s\theta & 0 \\ c\theta s\theta & s^2\theta & 0 \\ 0 & 0 & 0 \end{bmatrix}$$

$$\tilde{\Phi}_{v\omega}(\tau) = \tilde{\Phi}_{\omega v}^T(\tau) = \begin{bmatrix} c\theta \\ s\theta \\ 0 \end{bmatrix} \begin{bmatrix} -\Delta y \\ \Delta x \\ 1 \end{bmatrix}^T$$

$$\qquad (86)$$

$$= \begin{bmatrix} -c\theta \Delta y & c\theta \Delta x & c\theta \\ -s\theta \Delta y & s\theta \Delta x & s\theta \\ 0 & 0 & 0 \end{bmatrix}$$

$$\tilde{\Phi}_{\omega\omega}(\tau) = \begin{bmatrix} -\Delta y \\ \Delta x \\ 1 \end{bmatrix} \begin{bmatrix} -\Delta y \\ \Delta x \\ 1 \end{bmatrix}^T$$

$$= \begin{bmatrix} \Delta y^2 & -\Delta x \Delta y & -\Delta y \\ -\Delta x \Delta y & \Delta x^2 & \Delta x \\ -\Delta y & \Delta x & 1 \end{bmatrix}.$$

These appear in the error moment form of the general solution:

$$\delta \underline{x}(t) = \underline{IC}_d + \int_0^t \begin{bmatrix} c\theta \\ s\theta \\ 0 \end{bmatrix} \delta V d\tau + \int_0^t \begin{bmatrix} -\Delta y \\ \Delta x \\ 1 \end{bmatrix} \delta \omega d\tau$$

$$P(t) = IC_s \qquad (87)$$

$$+ \int_0^t \begin{bmatrix} -2c\theta \Delta y & c\theta \Delta x - s\theta \Delta y & c\theta \\ c\theta \Delta x - s\theta \Delta y & 2s\theta \Delta x & s\theta \\ c\theta & s\theta & 0 \end{bmatrix} \sigma_{v\omega} d\tau$$
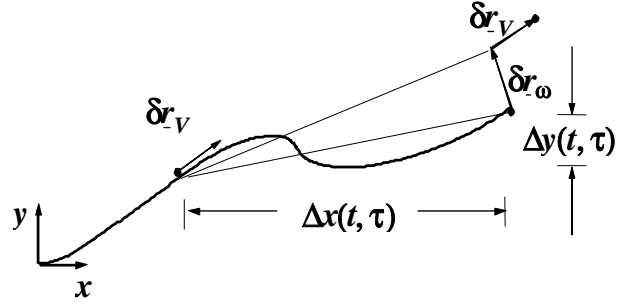

Fig. 4. Convolution integral.

$$+ \int_0^t \begin{bmatrix} c^2\theta & c\theta s\theta & 0 \\ c\theta s\theta & s^2\theta & 0 \\ 0 & 0 & 0 \end{bmatrix} \sigma_{vv} d\tau$$

$$+ \int_0^t \begin{bmatrix} \Delta y^2 & -\Delta x \Delta y & -\Delta y \\ -\Delta x \Delta y & \Delta x^2 & \Delta x \\ -\Delta y & \Delta x & 1 \end{bmatrix} \sigma_{\omega\omega} d\tau.$$

7.2.4. Intuitive Interpretation

It is clear now that the solution could have been written by inspection. The initial conditions affect the endpoint error in a predictable manner and the remaining terms amount to an addition of the effects felt at the endpoint at time t of the linear and angular errors occurring at each time τ between the start and end as illustrated in Figure 4.

The matrix relating input systematic errors occurring at time τ to their later effect at time t is:

$$d \begin{bmatrix} \delta x(t) \\ \delta y(t) \\ \delta \theta(t) \end{bmatrix} = \begin{bmatrix} c\theta & -\Delta y(t,\tau) \\ s\theta & \Delta x(t,\tau) \\ 0 & 1 \end{bmatrix} \begin{bmatrix} \delta V(\tau) \\ \delta \omega(\tau) \end{bmatrix} d\tau. \qquad (88)$$

Therefore, the covariance relationship is

$$d \begin{bmatrix} \sigma_{xx}(t) & \sigma_{xy}(t) & \sigma_{x\theta}(t) \\ \sigma_{xy}(t) & \sigma_{yy}(t) & \sigma_{y\theta}(t) \\ \sigma_{x\theta}(t) & \sigma_{y\theta}(t) & \sigma_{\theta\theta}(t) \end{bmatrix}$$

$$= \begin{bmatrix} c\theta & -\Delta y(t,\tau) \\ s\theta & \Delta x(t,\tau) \\ 0 & 1 \end{bmatrix} \begin{bmatrix} \sigma_{vv} & \sigma_{v\omega} \\ \sigma_{v\omega} & \sigma_{\omega\omega} \end{bmatrix} \qquad (89)$$

$$\begin{bmatrix} c\theta & -\Delta y(t,\tau) \\ s\theta & \Delta x(t,\tau) \\ 0 & 1 \end{bmatrix} d\tau.$$

These expressions are exactly what eq. (83) is integrating. The key assumption required to produce the solution by inspection is the common assumption of dynamics linearization,

that the reference trajectory need not be updated to reflect the compounding effect of the input error histories over time.

This result is easy to derive using the technique of Section 6.4. Consider three frames of reference denoted 0 for the origin, τ for a running frame somewhere along the trajectory, and t for the endpoint. The homogeneous transform for the end pose can be determined as the product of the two intermediate relationships, thus

$$T_t^0 = T_\tau^0 T_t^\tau.$$

Exposing the details of these matrices leads to

$$
\begin{aligned}
x_t^0 &= c\theta_\tau^0 x_t^\tau - s\theta_\tau^0 y_t^\tau + x_\tau^0 \\
y_t^0 &= s\theta_\tau^0 x_t^\tau + c\theta_\tau^0 y_t^\tau + y_\tau^0 \\
\theta_t^0 &= \theta_\tau^0 + \theta_t^\tau.
\end{aligned}
\tag{90}
$$

So, the transition matrix is immediate

$$
\Phi(t, \tau) = \frac{\partial \underline{x}(t)}{\partial \underline{x}(\tau)} = \begin{bmatrix} 1 & 0 & -\Delta y(t, \tau) \\ 0 & 1 & \Delta x(t, \tau) \\ 0 & 0 & 1 \end{bmatrix}
\tag{91}
$$

because

$$
\begin{aligned}
\Delta x(t, \tau) &= c\theta_\tau^0 x_t^\tau - s\theta_\tau^0 y_t^\tau \\
\Delta y(t, \tau) &= s\theta_\tau^0 x_t^\tau + c\theta_\tau^0 y_t^\tau.
\end{aligned}
\tag{92}
$$

7.3. Differential Heading Odometry

Differential heading odometry is a special case of integrated heading odometry where angular velocity is derived from the differential indications of wheel linear velocities and the wheel tread W. Let there be a left wheel and a right wheel on either side of the vehicle reference point as shown in Fig. 5.

While the solution can be formed using the wheel velocities as the inputs, this case will be formulated with an observer in order to illustrate the more general case where the measurements $\underline{z}(t)$ may depend nonlinearly on both the state and the input. Let the measurement vector be the velocities of the two wheels:

$$
\underline{z}(t) = \begin{bmatrix} r(t) & l(t) \end{bmatrix}^T.
\tag{93}
$$

7.3.1. Observer

The relationship between these and the equivalent integrated heading inputs is

$$
\underline{z}(t) = M\underline{u}(t) \quad \begin{bmatrix} r(t) \\ l(t) \end{bmatrix} = \begin{bmatrix} 1 & W/2 \\ 1 & -W/2 \end{bmatrix} \begin{bmatrix} V(t) \\ \omega(t) \end{bmatrix}.
\tag{94}
$$

This is a particularly simple version of the more general form of the observer in eq. (20). The inverse relationship is
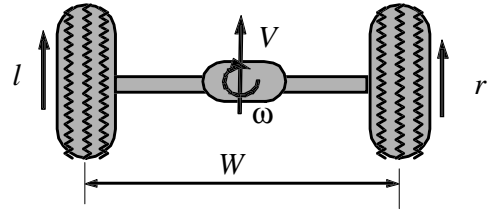

Fig. 5. Differential heading odometry.

immediate:

$$
\underline{u}(t) = M^{-1}\underline{z}(t) \quad \begin{bmatrix} V(t) \\ \omega(t) \end{bmatrix} = \begin{bmatrix} 1/2 & 1/2 \\ 1/W & -1/W \end{bmatrix} \begin{bmatrix} r(t) \\ l(t) \end{bmatrix}.
\tag{95}
$$

The observer Jacobians are

$$
H(t) = \begin{bmatrix} 0 & 0 & 0 \\ 0 & 0 & 0 \end{bmatrix} M(t) = N(t) = \begin{bmatrix} 1 & W/2 \\ 1 & -W/2 \end{bmatrix}.
\tag{96}
$$

Following eq. (28), the measurement spectral covariance R can be used instead of the process noise covariance Q by substituting the following for L:

$$
\tilde{L}(t) = LN^{-1} = \tilde{G}(t).
\tag{97}
$$

These new matrices are

$$
\begin{aligned}
\tilde{G}(t) = \tilde{L}(t) &= \begin{bmatrix} c\theta & 0 \\ s\theta & 0 \\ 0 & 1 \end{bmatrix} \begin{bmatrix} 1/2 & 1/2 \\ 1/W & -1/W \end{bmatrix} \\
&= \begin{bmatrix} c\theta/2 & c\theta/2 \\ s\theta/2 & s\theta/2 \\ 1/W & -1/W \end{bmatrix}.
\end{aligned}
$$

7.3.2. Transition Matrix

Therefore, the input transition matrix is

$$
\begin{aligned}
\tilde{\Phi}(t, \tau) = \Phi(t, \tau)\tilde{G}(t) &= \begin{bmatrix} 1 & 0 & -\Delta y(t, \tau) \\ 0 & 1 & \Delta x(t, \tau) \\ 0 & 0 & 1 \end{bmatrix} \\
&\quad \begin{bmatrix} c\theta & 0 \\ s\theta & 0 \\ 0 & 1 \end{bmatrix} \begin{bmatrix} 1/2 & 1/2 \\ 1/W & -1/W \end{bmatrix} \\
&= \begin{bmatrix} c\theta & -\Delta y(t, \tau) \\ s\theta & \Delta x(t, \tau) \\ 0 & 1 \end{bmatrix} \begin{bmatrix} 1/2 & 1/2 \\ 1/W & -1/W \end{bmatrix}.
\end{aligned}
\tag{98}
$$

The known errors can be converted to an equivalent set of errors in integrated heading:

$$
\begin{bmatrix} \delta V(t) \\ \delta \omega(t) \end{bmatrix}_{DH} = \begin{bmatrix} 1/2 & 1/2 \\ 1/W & -1/W \end{bmatrix} \begin{bmatrix} \delta r(t) \\ \delta l(t) \end{bmatrix}
$$

$$
\begin{bmatrix} \sigma_{vv} & \sigma_{v\omega} \\ \sigma_{v\omega} & \sigma_{\omega\omega} \end{bmatrix}_{DH} = \begin{bmatrix} \dfrac{1}{2} & \dfrac{1}{2} \\ \dfrac{1}{W} & -\dfrac{1}{W} \end{bmatrix} \begin{bmatrix} \sigma_{rr} & \sigma_{rl} \\ \sigma_{rl} & \sigma_{ll} \end{bmatrix} \begin{bmatrix} \dfrac{1}{2} & \dfrac{1}{2} \\ \dfrac{1}{W} & -\dfrac{1}{W} \end{bmatrix}^T .
$$
(99)

This transformation will introduce appropriate correlations between the linear and angular velocity uncertainties due to their common dependence on two other variables.

7.3.3. Solution in Matrix Form

Under this substitution, the solution is identical to the integrated heading case:

$$
\delta \underline{x}(t) = \underline{IC}_d + \int_0^t \begin{bmatrix} c\theta & -\Delta y(t, \tau) \\ s\theta & \Delta x(t, \tau) \\ 0 & 1 \end{bmatrix} \begin{bmatrix} \delta V(t) \\ \delta \omega(t) \end{bmatrix}_{DH} d\tau
$$

$$
P(t) = IC_s + \int_0^t \begin{bmatrix} c\theta & -\Delta y(t, \tau) \\ s\theta & \Delta x(t, \tau) \\ 0 & 1 \end{bmatrix}
$$

$$
\begin{bmatrix} \sigma_{vv} & \sigma_{v\omega} \\ \sigma_{v\omega} & \sigma_{\omega\omega} \end{bmatrix}_{DH} \begin{bmatrix} c\theta & -\Delta y(t, \tau) \\ s\theta & \Delta x(t, \tau) \\ 0 & 1 \end{bmatrix}^T d\tau .
$$
(100)

This result is the general linearized solution for the propagation of systematic and random error in 2D differential heading odometry for any trajectory and any error model. The conversion to an equivalent integrated heading problem will be carried out in every stage of subsequent derivations. It will later be necessary to convert the error models so that they are expressed in terms of equivalent integrated heading error inputs as well.

7.3.4. Solution in Error Moment Form

Under the transformation, the integrated heading result in eq. (87) applies equally to this case where the errors used are the integrated heading equivalents.

8. Error Models

The general solutions presented earlier are functions of both:

- the reference trajectory, as is characteristic of linear perturbations of nonlinear systems;

- the error models chosen.

In order to gain a deeper understanding of specific cases, these two choices must be made. Specific trajectories and error models will be assumed here in order to get specific results.

8.1. Error Gradient Notation

Error models such as constant biases and scale errors in the systematic case and time- or distance-dependent random walks in the random case will be used in examples. These assumptions will generate a large number of constants for which a consistent notation will be advisable. Most commonly, gradients of error with time, distance or angle will occur.

For systematic error, the partial derivative will be indicated by a right subscript. Thus:

$$
\delta V_v = \frac{\partial}{\partial V} \{\delta V\}.
$$

On the assumption that velocity sensor error is proportional to velocity, this error gradient is constant and

$$
\delta V = \delta V_v \times V.
$$

For random error, right subscripts are already used to indicate the variable operated upon by the variance operator. In this case the right bracketed superscript will be used. Thus:

$$
\sigma_{v\omega}^{(v)} = \frac{\partial}{\partial V} \{\sigma_{v\omega}\}.
$$

When this gradient is constant, the indicated covariance varies linearly with (usually unsigned) velocity:

$$
\sigma_{v\omega} = \sigma_{v\omega}^{(v)} \times |V|.
$$

8.2. Specific Error Models

For direct heading deterministic error, a speed encoder scale error (due, for example, to incorrect wheel radius) will be assumed. Likewise, a compass error due to a magnetic field produced by the vehicle will be assumed. For random error, a "motion-dependent" random walk (where variance grows linearly with distance rather than time) will be assumed. A constant spectral probability density for the compass leads to a time dependent random walk contribution to the position coordinates.

For integrated heading deterministic error, the same speed encoder scale error and a constant gyro bias will be assumed. For random error, a motion-dependent random walk encoder variance will be assumed as well as a constant gyro bias (in)stability.

For differential heading deterministic error, two potentially different encoder scale errors will be used. For random error, two potentially different motion dependent random walk variances will be assumed.

These assumptions are summarized in Table 1.

Table 1. Error Sources

Odometry Class	Deterministic Error Sources	Random Error Sources
Direct Heading	$\delta V = \delta V_v \times V$	$\sigma_{vv} = \sigma_{vv}^{(v)}|V|$
	$\delta \theta = \delta \theta_c \cos \theta + \delta \theta_s \sin \theta$	$\sigma_{\theta\theta} = const$
Integrated Heading	$\delta V = \delta V_v \times V$	$\sigma_{vv} = \sigma_{vv}^{(v)}|V|$
	$\delta \omega = const$	$\sigma_{\omega\omega} = const$
		$\sigma_{v\omega} = 0$
Differential Heading	$\delta r = \delta r_r \times r$	$\sigma_{rr} = \alpha_{rr}|V_r|$
	$\delta l = \delta l_l \times l$	$\sigma_{ll} = \alpha_{ll}|V_l|$
		$\sigma_{rl} = 0$

The constants $\delta\theta_c$ and $\delta\theta_s$ are not gradients but the components of the magnetic field generated by the vehicle resolved onto body fixed axes. The absolute value signs appear in order to enforce the condition that variance remains positive regardless of the direction of motion. Many stochastic error integrals over distance or angle must interpret the distance differentials ds and $d\theta$ in an unsigned fashion.

8.3. Equivalent Error Models

Equation (100) can be unwieldy in hand calculations. However, the differential heading errors can be converted to an equivalent set of integrated heading errors. Substituting the appropriate error models and eq. (95) into eq. (99) leads to the integrated heading error model which is equivalent to a given differential heading model. For systematic error:

$$\begin{bmatrix} \delta V(t) \\ \delta \omega(t) \end{bmatrix}_{DH} dt = \begin{bmatrix} \delta V_v V(t) \\ \delta \omega_v V(t) \end{bmatrix} dt = \begin{bmatrix} \delta V_v \\ \delta \omega_v \end{bmatrix} ds$$

$$\begin{bmatrix} \delta V(t) \\ \delta \omega(t) \end{bmatrix}_{DH} dt = \begin{bmatrix} \delta V_\omega \omega(t) \\ \delta \omega_\omega \omega(t) \end{bmatrix} dt = \begin{bmatrix} \delta V_\omega \\ \delta \omega_\omega \end{bmatrix} d\theta. \tag{101}$$

If $R(t)$ is the instantaneous radius of curvature, the derived equivalent gradients for systematic error are dependent on curvature and velocity:

$$\delta V_v(t)|_{DH} = \left\{ \left(\frac{\delta r_r + \delta l_l}{2} \right) + \frac{(\delta r_r - \delta l_l)}{4R(t)} W \right\}$$

$$\delta \omega_v(t)|_{DH} = \left\{ \frac{(\delta r_r - \delta l_l)}{W} + \left(\frac{\delta r_r + \delta l_l}{2R(t)} \right) \right\} \tag{102}$$

$$\delta V_\omega(t)|_{DH} = R(t)\delta V_v(t)|_{DH}$$

$$\delta \omega_\omega(t)|_{DH} = R(t)\delta \omega_v(t)|_{DH} .$$

These are time-dependent expressions but they are constant on a constant curvature trajectory when the original differential heading gradients were constant. In this case, it becomes possible to compute the error characteristics of a differential odometer which are equivalent to a given gyroscope, for example.

The two forms for distance and angle above can be used to remove the singularity when $R(t) = 0$ from error integrals by a change of variable, switching to the other form as necessary.

When applying the same procedure to stochastic error, it becomes necessary to enforce the condition that unsigned wheel velocities are used. A convenient way to do so is to define the equivalent linear and angular velocities by "manhattan" sums and differences thus:

$$\begin{bmatrix} V(t) \\ \omega(t) \end{bmatrix}_{DH} = \begin{bmatrix} 1/2 & 1/2 \\ 1/W & -1/W \end{bmatrix} \begin{bmatrix} |r(t)| \\ |l(t)| \end{bmatrix} = \begin{bmatrix} \dfrac{|r(t)| + |l(t)|}{2} \\ \dfrac{|r(t)| - |l(t)|}{W} \end{bmatrix}$$

$$\kappa(t)|_{DH} = \omega(t)|_{DH} / V(t)|_{DH} \tag{103}$$

$$R(t)|_{DH} = V(t)|_{DH} / \omega(t)|_{DH}.$$

For a straight trajectory, these give expected results, but note that in a point turn $V(t)|_{DH} \neq 0$ and $\omega(t)|_{DH} = 0$. The differentials ds and $d\theta$ must be interpreted in a manner consistent with these definitions. This device leads to the following equivalent random error models:

$$\begin{bmatrix} \sigma_{vv} & \sigma_{v\omega} \\ \sigma_{v\omega} & \sigma_{\omega\omega} \end{bmatrix}_{DH} dt = \begin{bmatrix} \sigma_{vv}^{(v)} & \sigma_{v\omega}^{(v)} \\ \sigma_{v\omega}^{(v)} & \sigma_{\omega\omega}^{(v)} \end{bmatrix} V(t)|_{DH}$$

$$dt = \begin{bmatrix} \sigma_{vv}^{(v)} & \sigma_{v\omega}^{(v)} \\ \sigma_{v\omega}^{(v)} & \sigma_{\omega\omega}^{(v)} \end{bmatrix} ds$$

$$\begin{bmatrix} \sigma_{vv} & \sigma_{v\omega} \\ \sigma_{v\omega} & \sigma_{\omega\omega} \end{bmatrix}_{DH} dt = \begin{bmatrix} \sigma_{vv}^{(\omega)} & \sigma_{v\omega}^{(\omega)} \\ \sigma_{v\omega}^{(\omega)} & \sigma_{\omega\omega}^{(\omega)} \end{bmatrix} \omega(t)|_{DH} \tag{104}$$

$$dt = \begin{bmatrix} \sigma_{vv}^{(v)} & \sigma_{v\omega}^{(v)} \\ \sigma_{v\omega}^{(v)} & \sigma_{\omega\omega}^{(v)} \end{bmatrix} d\theta.$$

The equivalent error gradients are

$$\sigma_{vv}^{(v)}(t)|_{DH} = \frac{\left(\sigma_{rr}^{(r)} + \sigma_{ll}^{(l)}\right)}{4} + \frac{\left(\sigma_{rr}^{(r)} - \sigma_{ll}^{(l)}\right)}{4} \frac{W}{2R(t)|_{DH}}$$

$$\sigma_{v\omega}^{(v)}|_{DH} = \frac{\left(\sigma_{rr}^{(r)} - \sigma_{ll}^{(l)}\right)}{2W} + \frac{\left(\sigma_{rr}^{(r)} + \sigma_{ll}^{(l)}\right)}{4R(t)|_{DH}} \tag{105}$$

$$\sigma_{\omega\omega}^{(v)}|_{DH} = \frac{\left(\sigma_{rr}^{(r)} + \sigma_{ll}^{(l)}\right)}{W^2} + \frac{\left(\sigma_{rr}^{(r)} - \sigma_{ll}^{(l)}\right)}{W^2}\frac{W}{2R(t)|_{DH}}$$

$$\sigma_{vv}^{(\omega)}(t)|_{DH} = R(t)|_{DH}\sigma_{vv}^{(v)}(t)|_{DH}$$

$$\sigma_{v\omega}^{(\omega)}(t)|_{DH} = R(t)|_{DH}\sigma_{v\omega}^{(v)}(t)|_{DH}$$

$$\sigma_{\omega\omega}^{(\omega)}(t)|_{DH} = R(t)|_{DH}\sigma_{\omega\omega}^{(v)}(t)|_{DH}.$$

When using the stochastic equivalents, it is important to interpret the equivalent linear and angular velocity in a manner consistent with the use of unsigned wheel velocities:

$$V(t)|_{DH} = (|V_r(t)| + |V_l(t)|)\,/2$$

$$\omega(t)|_{DH} = (|V_r(t)| - |V_l(t)|)\,/\,W$$

$$\kappa(t)|_{DH} = \omega(t)|_{DH}/\,V(t)|_{DH}$$

$$R(t)|_{DH} = V(t)|_{DH}/\omega(t)|_{DH}.$$

(106)

The second forms of the last three expressions are for convenience only since the equivalent radius can never vanish. Indeed for the stochastic constants:

$$|R(t)|_{DH}| \geq 1 \quad |\kappa(t)|_{DH}| \leq 1.$$

Also, the apparent singularity when both wheel velocities is zero is removable. Returning to the original form shows that the constants are zero under these circumstances.

8.4. Solutions in Terms of Trajectory Moment Matrices

Under the above error assumptions, (and the rare additional assumption of constant velocity and/or curvature) all earlier results can now be written in terms of trajectory moments. This step renders the results in essentially algebraic form since trajectory moments can be tabulated for specific trajectories.

8.4.1. Direct Heading Odometry

The direct heading linearized dynamics from eq. (74) are now

$$\frac{d}{dt}\begin{bmatrix} \delta x(t) \\ \delta y(t) \end{bmatrix} = \begin{bmatrix} 0 & 0 \\ 0 & 0 \end{bmatrix}\begin{bmatrix} \delta x(t) \\ \delta y(t) \end{bmatrix} + \begin{bmatrix} c\theta & -Vs\theta \\ s\theta & Vc\theta \end{bmatrix}$$

$$\begin{bmatrix} \delta V_v V \\ \delta\theta_c c\theta + \delta\theta_s s\theta \end{bmatrix}.$$

This can be rewritten as

$$\frac{d}{dt}\begin{bmatrix} \delta x(t) \\ \delta y(t) \end{bmatrix} = \begin{bmatrix} c\theta & -s\theta \\ s\theta & c\theta \end{bmatrix}\begin{bmatrix} \delta V_v \\ \delta\theta_c c\theta + \delta\theta_s s\theta \end{bmatrix}V$$

$$\frac{d}{ds}\begin{bmatrix} \delta x(s) \\ \delta y(s) \end{bmatrix} = \begin{bmatrix} c\theta & -s\theta \\ s\theta & c\theta \end{bmatrix}\begin{bmatrix} \delta V_v \\ \delta\theta_c c\theta + \delta\theta_s s\theta \end{bmatrix}.$$

(107)

Under this error model this system is now homogeneous to the first degree in the input velocity. This implies that systematic errors will be motion-dependent and reversible.

The direct heading solution from eq. (77) is now

$$\delta\underline{x}(s) = \begin{bmatrix} \delta x(0) \\ \delta y(0) \end{bmatrix} + \delta V_v \int_0^s \begin{bmatrix} c\theta \\ s\theta \end{bmatrix}ds$$

$$+ \int_0^s \begin{bmatrix} -\delta\theta_c s\theta c\theta - \delta\theta_s s^2\theta \\ \delta\theta_s s\theta c\theta + \delta\theta_c c^2\theta \end{bmatrix}ds$$

$$P(s) = P(0) + \sigma_{vv}^{(v)} \int_0^s \begin{bmatrix} c^2\theta & c\theta s\theta \\ c\theta s\theta & s^2\theta \end{bmatrix}ds$$

$$+ |V|\sigma_{\theta\theta}\int_0^2 \begin{bmatrix} s^2\theta & -c\theta s\theta \\ -c\theta s\theta & c^2\theta \end{bmatrix}ds.$$

(108)

The expression $|V|$ appears because it was necessary to factor

$$V^2dt = |V| \times |V|dt = |V| \times ds$$

in order to render ds unsigned.

Isolating the trajectory moment matrices and expressing them in terms of the scalar moment notation:

$$\delta\underline{x}(s) = \begin{bmatrix} \delta x(0) \\ \delta y(0) \end{bmatrix} + \delta V_v\begin{bmatrix} x(s) \\ y(s) \end{bmatrix} + \begin{bmatrix} -\delta\theta_c S_{sc}(s) - \delta\theta_s S_{ss}(s) \\ \delta\theta_s S_{sc}(s) + \delta\theta_c S_{cc}(s) \end{bmatrix}$$

$$P(s) = P(0) + \sigma_{vv}^{(v)}\begin{bmatrix} S_{cc}(s) & S_{sc}(s) \\ S_{sc}(s) & S_{ss}(s) \end{bmatrix}$$

$$+ |V|\sigma_{\theta\theta}\begin{bmatrix} S_{ss}(s) & -S_{sc}(s) \\ -S_{sc}(s) & S_{cc}(s) \end{bmatrix}.$$

(109)

All terms in this solution are motion-dependent so error propagation ceases when motion stops. Systematic error is reversible as expected. The arc length s is signed in the systematic case and unsigned in the stochastic case.

8.4.2. Integrated Heading Odometry

The integrated heading linearized dynamics from eq. (81) are now

$$\frac{d}{dt}\begin{bmatrix} \delta x(t) \\ \delta y(t) \\ \delta\theta(t) \end{bmatrix} = \begin{bmatrix} 0 & 0 & -Vs\theta \\ 0 & 0 & Vc\theta \\ 0 & 0 & 0 \end{bmatrix}\begin{bmatrix} \delta x(t) \\ \delta y(t) \\ \delta\theta(t) \end{bmatrix}$$

$$+ \begin{bmatrix} c\theta(t) & 0 \\ s\theta(t) & 0 \\ 0 & 1 \end{bmatrix}\begin{bmatrix} \delta V_v V \\ \delta\omega \end{bmatrix}.$$

(110)

Here, the growth of heading error depends fundamentally on time so this system is not motion-dependent.

The integrated heading solution from eq. (87) is

$$\delta\underline{x}(t) = \underline{IC}_d + \delta V_v \int_0^s \begin{bmatrix} c\theta \\ s\theta \\ 0 \end{bmatrix} ds + \delta\omega \int_0^t \begin{bmatrix} -\Delta y \\ \Delta x \\ 1 \end{bmatrix} d\tau$$

$$P(t) = IC_s + \sigma_{vv}^{(v)} \int_0^s \begin{bmatrix} c^2\theta & c\theta s\theta & 0 \\ c\theta s\theta & s^2\theta & 0 \\ 0 & 0 & 0 \end{bmatrix} ds \qquad (111)$$

$$+ \sigma_{\omega\omega} \int_0^t \begin{bmatrix} \Delta y^2 & -\Delta x\Delta y & -\Delta y \\ -\Delta x\Delta y & \Delta x^2 & \Delta x \\ -\Delta y & \Delta x & 1 \end{bmatrix} d\tau$$

Isolating the trajectory moment matrices and expressing them in terms of the scalar moment notation:

$$\delta\underline{x}(t) = \underline{IC}_d + \delta V_v \begin{bmatrix} S_c(s) \\ S_s(s) \\ 0 \end{bmatrix} + \delta\omega \begin{bmatrix} -T_y(t) \\ T_x(t) \\ t \end{bmatrix}$$

$$P(t) = IC_s + \sigma_{vv}^{(v)} \begin{bmatrix} S_{cc}(s) & S_{sc}(s) & 0 \\ S_{sc}(s) & S_{ss}(s) & 0 \\ 0 & 0 & 0 \end{bmatrix} \qquad (112)$$

$$+ \sigma_{\omega\omega} \begin{bmatrix} T_{yy}(t) & -T_{xy}(t) & -T_y(t) \\ -T_{xy}(t) & T_{xx}(t) & T_x(t) \\ -T_y(t) & T_x(t) & t \end{bmatrix}.$$

8.4.3. Differential Heading Odometry

The equivalent integrated heading linearized dynamics are obtained from eq. (81). The equivalent error gradients will henceforth drop the *DH* subscript. The equivalent linearized dynamics are now:

$$\frac{d}{t} \begin{bmatrix} \delta x(t) \\ \delta y(t) \\ \delta\theta(t) \end{bmatrix} = \begin{bmatrix} 0 & 0 & -Vs\theta \\ 0 & 0 & Vc\theta \\ 0 & 0 & 0 \end{bmatrix} \begin{bmatrix} \delta x(t) \\ \delta y(t) \\ \delta\theta(t) \end{bmatrix}$$

$$+ \begin{bmatrix} c\theta(t) & 0 \\ s\theta(t) & 0 \\ 0 & 1 \end{bmatrix} \begin{bmatrix} \delta V_v(t)V \\ \delta\omega(t) \end{bmatrix}. \qquad (113)$$

Recall from eq. (102) the definition of $\delta\omega_v(t)$ and $\delta\omega_\omega(t)$. Dividing respectively by V and ω gives the dynamics in the forms:

$$\frac{d}{ds} \begin{bmatrix} \delta x(s) \\ \delta y(s) \\ \delta\theta(s) \end{bmatrix} = \begin{bmatrix} 0 & 0 & -s\theta \\ 0 & 0 & c\theta \\ 0 & 0 & 0 \end{bmatrix} \begin{bmatrix} \delta x(s) \\ \delta y(s) \\ \delta\theta(s) \end{bmatrix}$$

$$+ \begin{bmatrix} c\theta(s) & 0 \\ s\theta(s) & 0 \\ 0 & 1 \end{bmatrix} \begin{bmatrix} \delta V_v(s) \\ \delta\omega_v(s) \end{bmatrix} \qquad (114)$$

$$\frac{d}{d\theta} \begin{bmatrix} \delta x(\theta) \\ \delta y(\theta) \\ \delta\theta(\theta) \end{bmatrix} = \begin{bmatrix} 0 & 0 & -Rs\theta \\ 0 & 0 & Rc\theta \\ 0 & 0 & 0 \end{bmatrix} \begin{bmatrix} \delta x(\theta) \\ \delta y(\theta) \\ \delta\theta(\theta) \end{bmatrix}$$

$$+ \begin{bmatrix} c\theta & 0 \\ s\theta & 0 \\ 0 & 1 \end{bmatrix} \begin{bmatrix} \delta V_\omega(s) \\ \delta\omega_\omega(s) \end{bmatrix}.$$

So this system is motion-dependent and, when turning, the independent variable can be changed to heading angle. The differential heading solution from eq. (100) is now

$$\delta\underline{x}(s) = \underline{IC}_d + \int_0^s \delta V_v(s) \begin{bmatrix} c\theta \\ s\theta \\ 0 \end{bmatrix} ds + \int_0^s \delta\omega_v(s) \begin{bmatrix} -\Delta y \\ \Delta x \\ 1 \end{bmatrix} ds$$

$$P(s) = IC_s$$

$$+ \int_0^s \begin{bmatrix} -2c\theta\Delta y & c\theta\Delta x - s\theta\Delta y & c\theta \\ c\theta\Delta x - s\theta\Delta y & 2s\theta\Delta x & s\theta \\ c\theta & s\theta & 0 \end{bmatrix} \sigma_{v\omega}^{(v)}(s)ds$$

$$+ \int_0^s \begin{bmatrix} c^2\theta & c\theta s\theta & 0 \\ c\theta s\theta & s^2\theta & 0 \\ 0 & 0 & 0 \end{bmatrix} \sigma_{vv}^{(v)}(s)ds \qquad (115)$$

$$+ \int_0^s \begin{bmatrix} \Delta y^2 & -\Delta x\Delta y & -\Delta y \\ -\Delta x\Delta y & \Delta x^2 & \Delta x \\ -\Delta y & \Delta x & 1 \end{bmatrix} \sigma_{\omega\omega}^{(v)}(s)ds.$$

All terms in this solution are motion-dependent as expected. The covariance integrals must be interpreted carefully to ensure that the error accumulation is consistent with unsigned wheel velocities. When the trajectory is of constant curvature, the trajectory moment matrices can be isolated and expressed in terms of the scalar moment notation:

$$\delta\underline{x}(s) = \underline{IC}_d + \delta V_v \begin{bmatrix} S_c(s) \\ S_s(s) \\ 0 \end{bmatrix} + \delta\omega_v \begin{bmatrix} -S_y(s) \\ S_x(s) \\ s \end{bmatrix}$$

$$P(t) = IC_s$$

$$+ \sigma_{v\omega}^{(v)} \begin{bmatrix} -2S_{yc}(s) & S_{xc}(s) - S_{ys}(s) & S_c(s) \\ S_{xc}(s) - S_{ys}(s) & 2S_{xs}(s) & S_s(s) \\ S_c(s) & S_s(s) & 0 \end{bmatrix}$$

$$+ \sigma_{vv}^{(v)} \begin{bmatrix} S_{cc}(s) & S_{sc}(s) & 0 \\ S_{sc}(s) & S_{ss}(s) & 0 \\ 0 & 0 & 0 \end{bmatrix} \qquad (116)$$

$$+ \sigma_{\omega\omega}^{(v)} \begin{bmatrix} S_{yy}(s) & -S_{xy}(s) & -S_y(s) \\ -S_{xy}(s) & S_{xx}(s) & S_x(s) \\ -S_y(s) & S_x(s) & s \end{bmatrix}.$$

The extra matrix associated with $\sigma_{v\omega}^{(v)}$ arises from the fact that the errors in linear and angular velocities are correlated due to their common basis on two underlying measurements of wheel velocities.

The alternative form is also available:

$$\delta \underline{x}(\theta) = \underline{IC}_d + \int_0^\theta \delta V_\omega(\theta) \begin{bmatrix} c\theta \\ s\theta \\ 0 \end{bmatrix} d\theta + \int_0^\theta \delta \omega_\omega(\theta) \begin{bmatrix} -\Delta y \\ \Delta x \\ 1 \end{bmatrix} d\theta$$

$$P(\theta) = IC_s$$

$$+ \int_0^\theta \begin{bmatrix} -2c\theta\,\Delta y & c\theta\,\Delta x - s\theta\,\Delta y & c\theta \\ c\theta\,\Delta x - s\theta\,\Delta y & 2s\theta\,\Delta x & s\theta \\ c\theta & s\theta & 0 \end{bmatrix} \sigma_{v\omega}^{(\omega)}(\theta)d\theta$$

$$+ \int_0^\theta \begin{bmatrix} c^2\theta & c\theta s\theta & 0 \\ c\theta s\theta & s^2\theta & 0 \\ 0 & 0 & 0 \end{bmatrix} \sigma_{vv}^{(\omega)}(\theta)d\theta \qquad (117)$$

$$+ \int_0^\theta \begin{bmatrix} \Delta y^2 & -\Delta x\,\Delta y & -\Delta y \\ -\Delta x\,\Delta y & \Delta x^2 & \Delta x \\ -\Delta y & \Delta x & 1 \end{bmatrix} \sigma_{\omega\omega}^{(\omega)}(\theta)d\theta.$$

When the trajectory is of constant curvature, the trajectory moment matrices can be isolated and expressed in terms of the scalar moment notation:

$$\delta \underline{x}(\theta) = \underline{IC}_d + \delta V_\omega \begin{bmatrix} \Theta_c(\theta) \\ \Theta_s(\theta) \\ 0 \end{bmatrix} + \delta \omega_\omega \begin{bmatrix} -\Theta_y(\theta) \\ \Theta_x(\theta) \\ \theta \end{bmatrix}$$

$$P(\theta) = IC_s$$

$$+ \sigma_{v\omega}^{(\omega)} \begin{bmatrix} -2\Theta_{yc}(\theta) & \Theta_{xc}(\theta) - \Theta_{ys}(\theta) & \Theta_c(\theta) \\ \Theta_{xc}(\theta) - \Theta_{ys}(\theta) & 2\Theta_{xs}(\theta) & \Theta_s(\theta) \\ \Theta_c(\theta) & \Theta_s(\theta) & 0 \end{bmatrix}$$

$$+ \sigma_{vv}^{(\omega)} \begin{bmatrix} \Theta_{cc}(\theta) & \Theta_{sc}(\theta) & 0 \\ \Theta_{sc}(\theta) & \Theta_{ss}(\theta) & 0 \\ 0 & 0 & 0 \end{bmatrix} \qquad (118)$$

$$+ \sigma_{\omega\omega}^{(\omega)} \begin{bmatrix} \Theta_{yy}(\theta) & -\Theta_{xy}(\theta) & -\Theta_y(\theta) \\ -\Theta_{xy}(\theta) & \Theta_{xx}(\theta) & \Theta_x(\theta) \\ -\Theta_y(\theta) & \Theta_x(\theta) & \theta \end{bmatrix}.$$

9. Solutions on Particular Trajectories

Using the above assumed errors, error propagation is completely determined by the trajectory followed. This section gives closed-form propagation equations for linear, turn-in-place, and constant curvature trajectories. Trajectories will start from the origin facing along the x-axis. In this case, the term alongtrack refers to the direction parallel to the x-axis whereas the crosstrack direction is parallel to y.

9.1. Straight Trajectory

A linear trajectory, starting at the origin, parallel to the x-axis is defined by the following inputs:

$$\omega(t) = 0 \quad V(t) = \text{arbitrary}$$

and the associated solution to eq. (2):

$$x(t) = s(t) \quad y(t) = 0 \quad \theta(t) = 0. \qquad (119)$$

Error dynamics on this trajectory can also be used to approximate the local behavior of any trajectory up to the point where the deviation of the true trajectory from a straight one causes significant error in the Jacobians.

9.1.1. Direct Heading Odometry

The solution for direct heading from eq. (109) becomes

$$\delta \underline{x}(s) = \begin{bmatrix} \delta x(0) \\ \delta y(0) \end{bmatrix} + \delta V_v \begin{bmatrix} s \\ 0 \end{bmatrix} + \begin{bmatrix} 0 \\ \delta \theta_c s \end{bmatrix}$$

$$P(t) = P(0) + \sigma_{vv}^{(v)} \begin{bmatrix} s & 0 \\ 0 & 0 \end{bmatrix} + |V|\sigma_{\theta\theta} \begin{bmatrix} 0 & 0 \\ 0 & s \end{bmatrix}. \qquad (120)$$

Both translational deterministic errors are linear in distance, but for different reasons. The x error is due to the encoder scale error while the y error is due to the constant compass error at zero heading.

The covariance matrix remains diagonal. Alongtrack variance increases linearly with distance. Crosstrack variance also increases linearly under the assumption that velocity is constant.

9.1.2. Integrated Heading Odometry

The solution for integrated heading from eq. (112) becomes

$$\delta \underline{x}(t) = \underline{IC}_d + \delta V_v \begin{bmatrix} s(t) \\ 0 \\ 0 \end{bmatrix} + \delta \omega \begin{bmatrix} 0 \\ Vt^2/2 \\ t \end{bmatrix}$$

$$(t) = IC_s + \sigma_{vv}^{(v)} \begin{bmatrix} s & 0 & 0 \\ 0 & 0 & 0 \\ 0 & 0 & 0 \end{bmatrix} \qquad (121)$$

$$+ \sigma_{\omega\omega} \begin{bmatrix} 0 & 0 & 0 \\ 0 & (s^2 t)/3 & (st)/2 \\ 0 & (st)/2 & t \end{bmatrix}.$$

Constant velocity was assumed in getting the deterministic error term quadratic in time. Alongtrack error is linear in distance while heading error is linear in time. Crosstrack error includes a term linear in distance and another term which is quadratic in time or distance for constant velocity.

Constant velocity was assumed for the T_x and T_{xx} duration moments. Heading variance is linear in time as was intended. Heading covariance with crosstrack is linear in distance and time (or quadratic in either for constant velocity). Notice that the alongtrack variance is (to first order) linear in distance rather than time whereas crosstrack variance is cubic in time (or distance for constant velocity).

9.1.3. Differential Heading Odometry

The solution for differential heading from eq. (116) becomes

$$\delta\underline{x}(s) = \underline{IC}_d + \delta V_v(s)\begin{bmatrix} s \\ 0 \\ 0 \end{bmatrix} + \delta\omega_v(s)\begin{bmatrix} 0 \\ \frac{s^2}{2} \\ s \end{bmatrix}$$

$$P(s) = IC_s + \sigma_{v\omega}^{(v)}\begin{bmatrix} 0 & s^2/2 & s \\ s^2/2 & 0 & 0 \\ s & 0 & 0 \end{bmatrix}$$

$$+ \sigma_{vv}^{(v)}\begin{bmatrix} s & 0 & 0 \\ 0 & 0 & 0 \\ 0 & 0 & 0 \end{bmatrix} + \sigma_{\omega\omega}^{(v)}\begin{bmatrix} 0 & 0 & 0 \\ 0 & s^3/3 & s^2/2 \\ 0 & s^2/2 & s \end{bmatrix}.$$

(122)

All terms are motion-dependent. As in the integrated heading case, deterministic alongtrack error is linear in distance. However, in this case the heading error is also linear in distance (rather than time). The crosstrack error is quadratic in distance. Note that if s reverses, the entire error vector reverses, because all terms depend explicitly on s.

For random error, the expression $\sigma_{v\omega}^{(v)}$ vanishes (for straight trajectories) when both encoders have identical error statistics so the second term is due only to a differential in the characteristics of the encoder noises. When the encoders have identical noises, this solution is analogous (after replacing time with distance) to the integrated heading case. Heading variance and alongtrack variance are linear in distance whereas crosstrack variance is cubic.

9.2. Turn-In-Place Trajectory

A turn-in-place trajectory starting at the origin, parallel to the x-axis is defined by the following inputs:

$$\omega(t) = \textit{ arbitrary} \quad V(t) = 0$$

and the associated solution to eq. (2):

$$x(t) = 0 \quad y(t) = 0 \quad \theta(t) = \int_0^t \omega(t)dt.$$

(123)

9.2.1. Direct Heading Odometry

The solution for direct heading from eq. (109) becomes

$$\delta\underline{x}(s) = \begin{bmatrix} \delta x(0) \\ \delta y(0) \end{bmatrix} \quad P(s) = P(0).$$

(124)

Both translational deterministic errors are unchanged because no change in distance occurs. For random error, the covariance matrix is similarly unchanged. The solution means that encoder error is zero and compass error is irrelevant if the vehicle does not translate.

9.2.2. Integrated Heading Odometry

The solution for integrated heading from eq. (112) becomes

$$\delta\underline{x}(t) = \begin{bmatrix} \delta x(0) \\ \delta y(0) \\ \delta\theta(0) \end{bmatrix} + \delta\omega\begin{bmatrix} 0 \\ 0 \\ t \end{bmatrix}$$

$$P(t) = IC_s + \sigma_{\omega\omega}\begin{bmatrix} 0 & 0 & 0 \\ 0 & 0 & 0 \\ 0 & 0 & t \end{bmatrix}.$$

(125)

Deterministic translational error is unchanged and heading error increases linearly with time. For random error, all elements of covariance are unchanged with the exception of heading variance which grows linearly in time.

9.2.3. Differential Heading Odometry

For this trajectory, $R(t) = 0$ for the deterministic case. The distance-based equivalent error gradients such as $\delta V_v(t)$ are singular so this case is treated with the alternative angle form. The equivalent deterministic error gradients in eq. (102) become constants after removing the singularity

$$\delta V_\omega = R(t)\delta V_v(t) = \frac{(\delta r_r - \delta l_l)}{4}W$$

$$\delta\omega_\omega = R(t)\delta\omega_v(t) = \left(\frac{\delta r_r + \delta l_l}{2}\right).$$

For the stochastic case, $V(t)|_{DH} \neq 0$ and $\omega(t)|_{DH} = 0$ so $R(t)|_{DH}$ is singular. The stochastic solution comes from the distance-based forms and terms with $R(t)|_{DH}$ in their denominator vanish. The equivalent stochastic gradients from eq. (105) become distance-independent constants:

$$\sigma_{vv}^{(v)} = \frac{(\sigma_{rr}^{(r)} + \sigma_{ll}^{(l)})}{4}$$

$$\sigma_{v\omega}^{(v)} = \frac{(\sigma_{rr}^{(r)} - \sigma_{ll}^{(l)})}{2W}$$

$$\sigma_{\omega\omega}^{(v)} = \frac{(\sigma_{rr}^{(r)} + \sigma_{ll}^{(l)})}{W^2}.$$

Also, on this unique trajectory $\Delta x = \Delta y = 0$. The solution for differential heading, using the deterministic part of eq. (117) and the stochastic part of eq. (115) becomes

$$\delta\underline{x}(\theta) = \underline{IC}_d + \delta V_\omega \int_0^\theta \begin{bmatrix} c\theta \\ s\theta \\ 0 \end{bmatrix} d\theta + \delta\omega_\omega \int_0^\theta \begin{bmatrix} 0 \\ 0 \\ 1 \end{bmatrix} d\theta$$

$$P(s) = IC_s + \sigma_{v\omega}^{(v)} \int_0^s \begin{bmatrix} 0 & 0 & c\theta \\ 0 & 0 & s\theta \\ c\theta & s\theta & 0 \end{bmatrix} ds$$

$$+ \sigma_{vv}^{(v)} \int_0^s \begin{bmatrix} c^2\theta & c\theta s\theta & 0 \\ c\theta s\theta & s^2\theta & 0 \\ 0 & 0 & 0 \end{bmatrix} ds \qquad (126)$$

$$+ \sigma_{\omega\omega}^{(v)} \int_0^s \begin{bmatrix} 0 & 0 & 0 \\ 0 & 0 & 0 \\ 0 & 0 & 1 \end{bmatrix} ds$$

where the distance differential in the stochastic case is the total unsigned travel of both wheels.

$$ds = \left[\frac{|r(t)| + |l(t)|}{2} \right] dt.$$

All terms are motion-dependent. In this equivalent form, the integrals can be readily evaluated in closed form.

Deterministic translational errors are trig functions of the rotation scaled by the difference in encoder scale errors. Heading error is proportional to the average encoder scale error.

For random error, elements of the covariance matrix are trig functions scaled by either the difference between encoder noises or their average.

9.3. Constant Curvature Trajectory

A constant curvature (arc) trajectory, starting at the origin, initially parallel to the x-axis is defined by the following inputs

$$\omega(t) = \kappa(t)V(t) = V(t)/R$$

$$V(t) = \text{ arbitrary}$$

and the associated solution to eq. (2):

$$\theta(s) = \kappa s$$

$$x(s) = R\sin(\kappa s)$$

$$y(s) = R[1 - \cos(\kappa s)].$$

Also we define for later

$$T = 1/\omega.$$

9.3.1. Direct Heading Odometry

The solution for direct heading from eq. (109) becomes

$$\delta\underline{x}(s) = \begin{bmatrix} \delta x(0) \\ \delta y(0) \end{bmatrix} + \delta V_v \begin{bmatrix} x(s) \\ y(s) \end{bmatrix}$$

$$+ R \begin{bmatrix} -\delta\theta_c/4 \\ \delta\theta_s/4 \end{bmatrix} + \frac{1}{2} \begin{bmatrix} \delta\theta_s s \\ \delta\theta_c s \end{bmatrix}$$

$$+ \frac{R}{4} \begin{bmatrix} \delta\theta_c c2\theta + \delta\theta_s s2\theta \\ -\delta\theta_s c2\theta + \delta\theta_c s2\theta \end{bmatrix}$$

$$\qquad (127)$$

$$P(t) = P(0) + \frac{\sigma_{vv}^{(v)} R}{2} \begin{bmatrix} \theta + \dfrac{s2\theta}{2} & s^2\theta \\ s^2\theta & \theta - \dfrac{s2\theta}{2} \end{bmatrix}$$

$$+ |V|\sigma_{\theta\theta} \begin{bmatrix} \theta - \dfrac{s2\theta}{2} & -s^2\theta \\ -s^2\theta & \theta + \dfrac{s2\theta}{2} \end{bmatrix}$$

where $\theta = \kappa s$.

For deterministic error, there are linear terms relating to position coordinates and distance traveled and pure oscillation terms cycling twice per orbit of a complete circle.

For random error, all elements exhibit second harmonic oscillation. The variances also have a linear term. There is a particular radius when

$$\frac{\sigma_{vv}^{(v)} R}{2} = |V|\sigma_{\theta\theta}$$

where the principal variances become purely linear and all oscillations cancel.

9.3.2. Integrated Heading Odometry

The solution for integrated heading becomes

$$\delta\underline{x}(t) = \underline{IC}_d + \delta V_v \underline{f}_v + \delta\omega \underline{f}_\omega$$

$$P(t) = IC_s + \sigma_{vv}^{(v)} \boldsymbol{F}_{vv} + \sigma_{\omega\omega} \boldsymbol{F}_{\omega\omega}$$

$$\qquad (128)$$

where

$$\underline{f}_v = \begin{bmatrix} x \\ y \\ 0 \end{bmatrix} \qquad (129)$$

$$\underline{f}_\omega = \begin{bmatrix} -\dfrac{R}{\omega}[s\theta - \theta c\theta] \\ \dfrac{R}{\omega}[\theta s\theta + c\theta - 1] \\ t \end{bmatrix} = \begin{bmatrix} -(Tx(t) + t[y(t) - R]) \\ tx(t) - Ty(t) \\ t \end{bmatrix}.$$

The first moment matrix is

$$
\boldsymbol{F}_{vv} = \begin{bmatrix} R\left[\dfrac{\theta}{2}+\dfrac{s2\theta}{4}\right] & \dfrac{Rs^2\theta}{2} & 0 \\[2mm] \dfrac{Rs^2\theta}{2} & R\left[\dfrac{\theta}{2}-\dfrac{s2\theta}{4}\right] & 0 \\[2mm] 0 & 0 & 0 \end{bmatrix}
$$

$$
\boldsymbol{F}_{vv} = \begin{bmatrix} \dfrac{s}{2}+\dfrac{x}{2}\left(1-\dfrac{y}{R}\right) & \dfrac{x^2}{2R} & 0 \\[2mm] \dfrac{x^2}{2R} & \dfrac{s}{2}-\dfrac{x}{2}\left(1-\dfrac{y}{R}\right) & 0 \\[2mm] 0 & 0 & 0 \end{bmatrix}.
$$

(130)

The second moment matrix is

$$
\boldsymbol{F}_{\omega\omega} = \begin{bmatrix} \dfrac{R^2}{\omega}\left[\theta\left(1+\dfrac{c2\theta}{2}\right)-\dfrac{3}{2}\left(\dfrac{s2\theta}{2}\right)\right] \\[3mm] \dfrac{R^2}{\omega}\left[\theta\left(\dfrac{s2\theta}{2}\right)+\dfrac{3}{2}\left(\dfrac{c2\theta}{2}\right)-c\theta+\dfrac{1}{4}\right] \\[3mm] -\dfrac{R}{\omega}[s\theta-\theta c\theta] \end{bmatrix}
$$

$$
\begin{bmatrix} -\dfrac{R^2}{\omega}\left[\theta\left(\dfrac{s2\theta}{2}\right)+\dfrac{3}{2}\left(\dfrac{c2\theta}{2}\right)-c\theta+\dfrac{1}{4}\right] \\[3mm] \dfrac{R^2}{\omega}\left[\theta\left(1-\dfrac{c2\theta}{2}\right)+\dfrac{3}{2}\left(\dfrac{s2\theta}{2}\right)-2s\theta\right] \\[3mm] \dfrac{R}{\omega}[\theta s\theta+c\theta-1] \end{bmatrix}
$$

$$
\begin{bmatrix} -\dfrac{R}{\omega}[s\theta-\theta c\theta] \\[3mm] \dfrac{R}{\omega}[\theta s\theta+c\theta-1] \\[3mm] t \end{bmatrix}
$$

(matrices written by column)   (131)

$$
\boldsymbol{F}_{\omega\omega} = \begin{bmatrix} t\left(\dfrac{R^2}{2}+(R-y)^2\right)-3Tx\left(\dfrac{R}{2}-\dfrac{y}{2}\right) \\[3mm] -\left(xt(y-R)+T\left(\dfrac{3}{2}x^2-Ry\right)\right) \\[3mm] -(Tx(t)+t[y(t)-R]) \end{bmatrix}
$$

$$
\begin{bmatrix} -\left(xt(y-R)+T\left(\dfrac{3}{2}x^2-Ry\right)\right) \\[3mm] T_{xx}(t) \\[3mm] T_x(t) \end{bmatrix}
$$

$$
\begin{bmatrix} -(Tx(t)+t[y(t)-R]) \\[3mm] T_x(t) \\[3mm] t \end{bmatrix}.
$$

For systematic error, constant velocity was assumed for all duration moments. The heading error is linear in time whereas the position errors are entirely oscillatory and of increasing amplitude as time increases. The linear increase in amplitude is a first-order approximation to the true nonlinear behavior of

a beat frequency. Eventually, the amplitude decreases again in the exact nonlinear solution.

For random error, heading variance increases linearly with time as was intended. Covariances of translation with heading exhibit a sum of constant and linearly increasing oscillations at the fundamental frequency. Translational covariances include a constant oscillation at the fundamental and constant and linearly increasing oscillations at the second harmonic frequency. The translational variances include similar oscillatory terms and a pure linear term caused by both the gyro and the encoder variances.

9.3.3. Differential Heading Odometry

The solution for differential heading becomes

$$
\delta\underline{x}(t) = \underline{IC}_d + \delta V_v \underline{f}_v + \delta\omega \underline{f}_\omega
$$
$$
P(t) = IC_s + \sigma_{vv}^{(v)}\boldsymbol{F}_{vv} + \sigma_{v\omega}\boldsymbol{F}_{v\omega} + \sigma_{\omega\omega}\boldsymbol{F}_{\omega\omega}
$$

(132)

where

$$
\underline{f}_v = \begin{bmatrix} x(s) \\ y(s) \\ 0 \end{bmatrix}
$$

$$
\underline{f}_\omega = \begin{bmatrix} -R^2[s\theta-\theta c\theta] \\ R^2[\theta s\theta+c\theta-1] \\ s \end{bmatrix}
$$

$$
= \begin{bmatrix} -(Rx(s)+s[y(s)-R]) \\ sx(s)-Ry(s) \\ s \end{bmatrix}.
$$

(133)

For the stochastic integrals, the differential ds is based on the equivalent velocity:

$$
V|_{DH} = (|V_r|+|V_l|)/2.
$$

The first moment matrix is the same as the integrated heading case:

$$
\boldsymbol{F}_{vv} = \begin{bmatrix} R\left[\dfrac{\theta}{2}+\dfrac{s2\theta}{4}\right] & \dfrac{Rs^2\theta}{2} & 0 \\[2mm] \dfrac{Rs^2\theta}{2} & R\left[\dfrac{\theta}{2}-\dfrac{s2\theta}{4}\right] & 0 \\[2mm] 0 & 0 & 0 \end{bmatrix}
$$

$$
\boldsymbol{F}_{vv} = \begin{bmatrix} \dfrac{s}{2}+\dfrac{x}{2}\left(1-\dfrac{y}{R}\right) & \dfrac{x^2}{2R} & 0 \\[2mm] \dfrac{x^2}{2R} & \dfrac{s}{2}-\dfrac{x}{2}\left(1-\dfrac{y}{R}\right) & 0 \\[2mm] 0 & 0 & 0 \end{bmatrix}.
$$

(134)

The second moment matrix is

$$
\boldsymbol{F}_{v\omega} = \begin{bmatrix} -2R^2\left[\dfrac{\theta}{2} - \dfrac{s2\theta}{4}\right] & -R^2\left(\dfrac{1}{2} - c\theta + \dfrac{c2\theta}{2}\right) & Rs\theta \\ -R^2\left(\dfrac{1}{2} - c\theta + \dfrac{c2\theta}{2}\right) & 2R^2\left[\dfrac{\theta}{2} + s\theta - \dfrac{s2\theta}{4}\right] & R(1 - c\theta) \\ Rs\theta & R(1 - c\theta) & 0 \end{bmatrix}
$$

$$
\boldsymbol{F}_{v\omega} = \begin{bmatrix} -2\left(\dfrac{x}{2}(R - y) + R\left(\dfrac{s}{2}\right)\right) & \dfrac{1}{2}\left(x^2 - y^2\right) & x \\ \dfrac{1}{2}\left(x^2 - y^2\right) & R\left(-\dfrac{s}{2} + x\right) - \dfrac{x}{2}(R - y) & y \\ x & y & 0 \end{bmatrix}.
$$
(135)

The third moment matrix is

$$
\boldsymbol{F}_{\omega\omega} = \begin{bmatrix} \dfrac{R^2}{\kappa}\left[\theta\left(1 + \dfrac{c2\theta}{2}\right) - \dfrac{3}{2}\left(\dfrac{s2\theta}{2}\right)\right] \\ \dfrac{R^2}{\kappa}\left[\theta\left(\dfrac{s2\theta}{2}\right) + \dfrac{3}{2}\left(\dfrac{c2\theta}{2}\right) - c\theta + \dfrac{1}{4}\right] \\ -R^2\left[s\theta - \theta c\theta\right] \end{bmatrix}
$$

$$
\begin{bmatrix} \dfrac{R^2}{\kappa}\left[\theta\left(\dfrac{s2\theta}{2}\right) + \dfrac{3}{2}\left(\dfrac{c2\theta}{2}\right) - c\theta + \dfrac{1}{4}\right] \\ \dfrac{R^2}{\kappa}\left[\theta\left(1 - \dfrac{c2\theta}{2}\right) + \dfrac{3}{2}\left(\dfrac{s2\theta}{2}\right) - 2s\theta\right] \\ R^2\left[\theta s\theta + c\theta - 1\right] \end{bmatrix}
$$

$$
\begin{bmatrix} -R^2\left[s\theta - \theta c\theta\right] \\ R^2\left[\theta s\theta + c\theta - 1\right] \\ R\theta \end{bmatrix}
$$

(matrices written by column)   (136)

$$
\boldsymbol{F}_{\omega\omega} = \begin{bmatrix} s\left(\dfrac{R^2}{2} + (R - y)^2\right) - 3xR\left(\dfrac{R}{2} - \dfrac{y}{2}\right) \\ -\left(xs(y - R) + R\left(\dfrac{3}{2}x^2 - Ry\right)\right) \\ -(Rx(s) + s[y(s) - R]) \end{bmatrix}
$$

$$
\begin{bmatrix} -\left(xs(y - R) + R\left(\dfrac{3}{2}x^2 - Ry\right)\right) \\ s\left(\dfrac{R^2}{2} + x^2\right) - Rx\left(\dfrac{R}{2} - \dfrac{3y}{2}\right) \\ sx(s) - Ry(s) \end{bmatrix}
$$

$$
\begin{bmatrix} -(Rx(s) + s[y(s) - R]) \\ sx(s) - Ry(s) \\ s \end{bmatrix}.
$$

The structure is analogous to the integrated heading case. Deterministic heading error is linear in distance whereas the position errors are entirely oscillatory but of increasing amplitude as distance increases.

Heading variance increases linearly with distance as was intended. Covariances of translation with heading exhibit a sum of constant and linearly increasing oscillations at the fundamental frequency. Translational covariances include a constant oscillation at the fundamental and constant and linearly
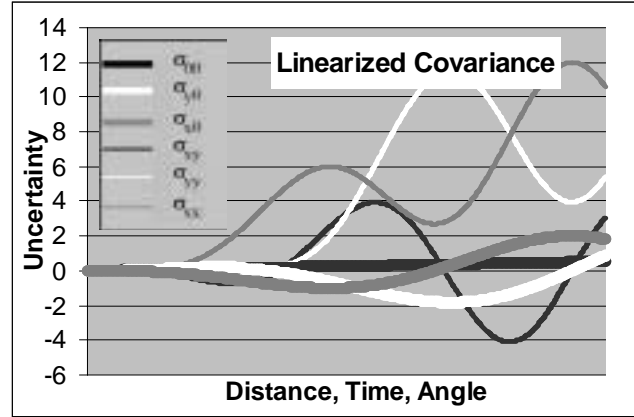

Fig. 6. Stochastic differential heading odometry error on an arc trajectory.

increasing oscillations at the second harmonic frequency. The translational variances include similar oscillatory terms and a pure linear term caused by both the mean and differential encoder variances.

For illustration purposes, the time evolution of the elements of the state covariance are provided in Figure 6. The vehicle speed is 0.25 m s^{-1} and the variance for both wheels advances at a rate of 1% of distance. The wheelbase is 1 m and the turn radius is 4 m. The total duration of the graph is 110 s comprising a total rotation of just over one revolution.

10. Applications

The results developed here have many practical uses in addition to their pedagogic value. This section presents some examples of problems that can be solved with the linearized theory of odometry error propagation.

10.1. Optimal Trajectories

Given results which express errors as functionals evaluated over a reference trajectory, it seems natural to wonder whether the calculus of variations can provide explicit results for those reference trajectories which are extremals of error. For example, optimal control theory could be used to try to find the input $\underline{u}(t)$ associated with extreme values of systematic error.

The formulation can be accomplished by adjoining the state and its perturbation and forming the functional

$$
J = \delta\underline{x}(t_f)^T \delta\underline{x}(t_f)
$$

subject to the constraints

$$
\begin{bmatrix} \dot{\underline{x}} \\ \dot{\delta\underline{x}} \end{bmatrix} = \begin{bmatrix} f(\underline{x}(t), \underline{u}(t), t) \\ F[.]\delta\underline{x} + G[.]\delta\underline{u} \end{bmatrix} \quad \begin{bmatrix} \underline{x}(t_0) \\ \delta\underline{x}(t_0) \end{bmatrix} \text{ given.}
$$

The Hamiltonian takes the form

$$H[\underline{x}(t), \underline{u}(t), \underline{\lambda}(t), t] = \underline{\lambda}^T(t) \underline{f}[\underline{x}(t), \underline{u}(t), \underline{\lambda}(t), t]$$

where $\underline{\lambda}(t)$ are time-varying Lagrange multiplier functions. The optimality condition is

$$\frac{\partial H}{\partial u} = \frac{\partial \underline{f}^T}{\partial u} \underline{\lambda} = 0.$$

This condition provides the differential equation that must be satisfied by solution at a stationary point of the performance index. Unfortunately in this case, the system dynamics are linear in the inputs (but recall the benefits of homogeneity) and the resulting optimality condition is not a differential equation but an implicit function which cannot be satisfied by nontrivial inputs.

Similarly, the problem can be attacked in a different manner by assuming trajectory moment matrices can be used (simple error models). For example, consider the following two moment matrices associated with random encoder and gyro errors:

$$\boldsymbol{F}_{vv} = \begin{bmatrix} S_{cc}(s) & S_{sc}(s) & 0 \\ S_{sc}(s) & S_{ss}(s) & 0 \\ 0 & 0 & 0 \end{bmatrix}$$

$$\boldsymbol{F}_{\omega\omega} = \begin{bmatrix} S_{yy}(s) & -S_{xy}(s) & -S_y(s) \\ -S_{xy}(s) & S_{xx}(s) & S_x(s) \\ -S_y(s) & S_x(s) & s \end{bmatrix}.$$

(137)

Consider these to be covariance matrices. The total variance provides a convenient performance index for optimization.

The trace of $\boldsymbol{F}_{vv}$ is

$$S_{cc}(s) + S_{ss}(s) = \int_0^s \left[c^2\theta + s^2\theta \right] ds = s.$$

Therefore, for a given endpoint, the shortest path has minimum variance and this is shown in the calculus of variations to be a straight line.

Concentrating on position error, the trace of the first two elements of $\boldsymbol{F}_{\omega\omega}$ is

$$S_{xx}(s) + S_{yy}(s) = \int_0^s \left[\Delta y^2 + \Delta x^2 \right] ds = \int_0^s \Delta R^2 ds$$

where ΔR is the radius from the endpoint to the historical point associated with the distance s. The integral is invariant to translations of coordinates so the endpoint can be set to the origin and the limits reversed to get the functional:

$$J = \int_0^s \left[x^2(\xi) + y^2(\xi) \right] d\xi.$$

The Euler–Lagrange equations of the calculus of variations applied to this parametric form of functional are

$$\frac{dJ}{ds} x'(s) = J_{x(s)} \quad \frac{dJ}{ds} y'(s) = J_{y(s)}.$$

Here, because the integrands contain no derivatives, the equations are again not differential equations and no stationary point exists.

However, it is easy to see that a boundary point extremum does exist. The integral is also invariant to rotations of coordinates, so let the endpoint be placed on the x-axis. The minimization problem is now

$$J = \int_0^s \left[x^2(s) + y^2(s) \right] ds \quad x(s) \text{ given}, y(s) = 0.$$

This integral is bounded from below and the bound is attainable from the set of continuous curves because

$$\int_0^s \left[x^2(s) + y^2(s) \right] ds > \int_0^s x^2(s) ds.$$

Any curve other than the straight line has a larger value of the performance index, so the straight line is the minimum. It has been shown that straight-line trajectories are extremals of random error in integrated heading odometry even though variational methods were of little assistance. The present theory contributes this result by supplying the explicit form of the performance index as the trace of a trajectory moment matrix.

10.2. Lateral Slip

Earlier sections have dealt with the case of systematic encoder scale error, symbolized by δV_v. Scale error was chosen to designate this case because variations in wheel radius, longitudinal slip and longitudinal skid all contribute to this error in a manner which is indistinguishable.

Of course, wheels often slip sideways, particularly when turning sharply. Consider an Ackerman steer vehicle, modeled by bicycle kinematics as shown in Figure 7.

The lateral slip angle for a wheel is the difference between where the wheel points and where it goes. Steer angle can be viewed as an indication of curvature because for small steer angles:

$$\gamma = \text{atan}\left(\frac{L}{R}\right) \approx \frac{L}{R} = \kappa L.$$

Odometry can be formulated using this measurement relationship, but for the present purpose it is economical to note that if slip can be assumed to be proportional to steer angle, then
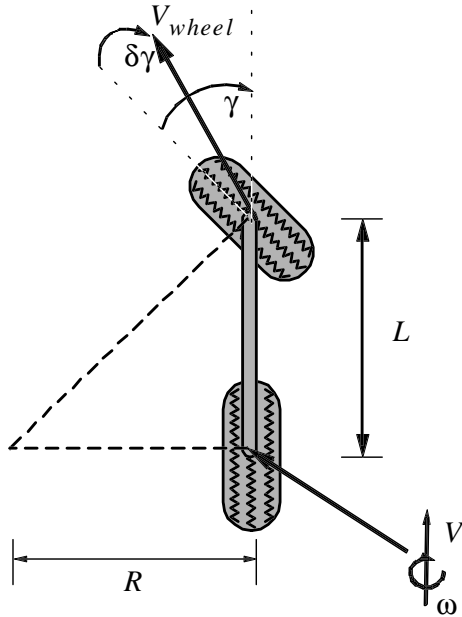
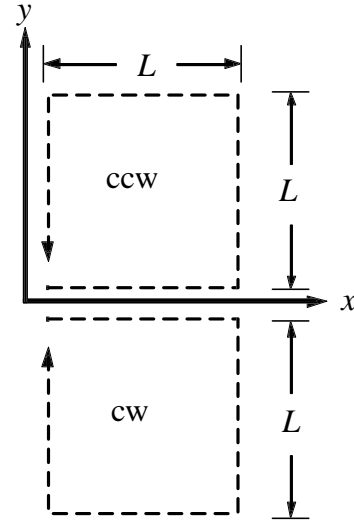Fig. 7. Lateral wheel slip in automotive applications.

Fig. 8. Test trajectories for UMBmark. The vehicle is driven over two closed trajectories and the closure error of the computed trajectory is used to calibrate systematic errors.

$$\delta\omega = \delta(\kappa V) = \delta\left(\frac{\gamma V}{L}\right) = \frac{V}{L}\delta\gamma$$

$$= \delta\gamma_\gamma\left(\frac{V}{L}\gamma\right) = \delta\gamma_\gamma\omega.$$

Hence, lateral wheel slip acts like a scale error in angular velocity. The associated differential error is of the form

$$\delta\omega dt = \delta\gamma_\gamma\omega dt = \delta\gamma_\gamma d\theta.$$

Given that angular velocity indications evolve according to the spatial moments, this result means that while spatial duration moments apply to gyro biases, spatial rotation moments apply to lateral wheel slip and gyro scale errors.

10.3. Calibration

Explicit expressions for the systematic and random errors that result from a given trajectory and error source are valuable in calibration applications. In principle, a vehicle can be driven over any known trajectory and the observed errors at the endpoint can be used to solve for the parameters of the assumed error source. In practice, generating many observations over the same trajectory is advisable in order to distinguish the mean (systematic) error from its variance.

Consider the calibration procedure, developed for differential heading odometry, known as the University of Michigan odometry benchmark (UMBmark) described in Borenstein

and Feng (1995). The vehicle is driven around two different paths designated the clockwise (CW) path and the counter-clockwise (CCW) path and returned to its initial heading as shown in Figure 8. The objective is to calibrate the difference in encoder scale factors (or wheel radii) and the wheel tread W. The two paths are illustrated in Figure 8.

10.3.1. Systematic Error

Perhaps the most straightforward procedure is to assume that the path length L is large relative to the wheel travel during the turns. Then, eq. (115) furnishes the error on the complete square trajectory in each direction. The result of the integration is

$$\delta\underline{x}(t)|_{ccw} = \delta\omega_v\begin{bmatrix} 2L^2 \\ -2L^2 \\ 4L \end{bmatrix} \quad \delta\underline{x}(t)|_{cw} = \delta\omega_v\begin{bmatrix} -2L^2 \\ -2L^2 \\ 4L \end{bmatrix}. \quad (138)$$

Errors due to the average encoder scale error are path-independent so they cancel out on these closed trajectories. To use these equations to calibrate systematic error, the endpoint error is measured directly and the equations are solved for the unknown $\delta\omega_v$. The six systematic error observations give rise to the system of equations:

$$\begin{bmatrix} \delta x_{ccw} \\ \delta y_{ccw} \\ \delta\theta_{ccw} \\ \delta x_{cw} \\ \delta y_{cw} \\ \delta\theta_{cw} \end{bmatrix} = \begin{bmatrix} 2L^2 \\ -2L^2 \\ 4L \\ -2L^2 \\ -2L^2 \\ 4L \end{bmatrix}\delta\omega_v. \quad (139)$$

This system is clearly of rank one. Maximum information can be extracted from a left pseudo-inverse solution. The systematic errors in x and y are equal due to the choice of a square trajectory. The four-component trajectories are straight so the angular error gradient from eq. (102) is

$$\delta\omega_v = \frac{(\delta r_r - \delta l_l)}{W}.$$

The three individual unknowns δr_r, δl_l, and W appear only in the form of this expression, so there is no way to solve for them independently. They could be resolved if the trajectories were not square and not closed (say, three sides of a rectangle).

10.3.2. Random Error

Neglecting the point turns, eq. (115) also furnishes the random error on the complete square trajectory in each direction. The result of the integration is

$$P(s)|_{ccw} = \sigma_{v\omega}^{(v)} \begin{bmatrix} -2L^2 & 0 & 0 \\ 0 & -2L^2 & 0 \\ 0 & 0 & 0 \end{bmatrix}$$

$$+ \sigma_{vv}^{(v)} \begin{bmatrix} 2L & 0 & 0 \\ 0 & 2L & 0 \\ 0 & 0 & 0 \end{bmatrix}$$

$$+ \sigma_{\omega\omega}^{(v)} \begin{bmatrix} \frac{5}{3}L^3 & -L^3 & 2L^2 \\ -L^3 & \frac{5}{3}L^3 & -2L^2 \\ 2L^2 & -2L^2 & 4L \end{bmatrix}$$

$$\hspace{6cm} (140)$$

$$P(s)|_{cw} = \sigma_{v\omega}^{(v)} \begin{bmatrix} 2L^2 & 0 & 0 \\ 0 & 2L^2 & 0 \\ 0 & 0 & 0 \end{bmatrix}$$

$$+ \sigma_{vv}^{(v)} \begin{bmatrix} 2L & 0 & 0 \\ 0 & 2L & 0 \\ 0 & 0 & 0 \end{bmatrix}$$

$$+ \sigma_{\omega\omega}^{(v)} \begin{bmatrix} \frac{5}{3}L^3 & L^3 & -2L^2 \\ L^3 & \frac{5}{3}L^3 & -2L^2 \\ -2L^2 & -2L^2 & 4L \end{bmatrix}.$$

On these straight trajectories, the error gradients from eq. (105) take the form

$$\sigma_{vv}^{(v)} = \frac{(\sigma_{rr}^{(r)} + \sigma_{ll}^{(l)})}{4}$$

$$\sigma_{v\omega}^{(v)} = \frac{(\sigma_{rr}^{(r)} - \sigma_{ll}^{(l)})}{2W}$$

$$\sigma_{\omega\omega}^{(v)} = \frac{(\sigma_{rr}^{(r)} + \sigma_{ll}^{(l)})}{W^2}.$$

A scatter matrix of observations can be formed from multiple trials. The observations on the counterclockwise trajectory give rise to the following system of equations:

$$\begin{bmatrix} \sigma_{xx} \\ \sigma_{yy} \\ \sigma_{xy} \\ \sigma_{x\theta} \\ \sigma_{y\theta} \\ \sigma_{\theta\theta} \end{bmatrix} = \begin{bmatrix} 2L & -2L^2 & \frac{5}{3}L^3 \\ 2L & -2L^2 & \frac{5}{3}L^3 \\ 0 & 0 & -L^3 \\ 0 & 0 & 2L^2 \\ 0 & 0 & -2L^2 \\ 0 & 0 & 4L \end{bmatrix} \begin{bmatrix} \sigma_{vv}^{(v)} \\ \sigma_{v\omega}^{(v)} \\ \sigma_{\omega\omega}^{(v)} \end{bmatrix}. \hspace{0.5cm} (141)$$

A similar set is formed from the counterclockwise trajectory. The above system is clearly only rank two, so the second trajectory is needed to completely determine the three unknowns. Once this occurs, the more fundamental three unknowns $\sigma_{rr}^{(r)}$, $\sigma_{ll}^{(l)}$, and W could be determined uniquely as well.

10.3.3. Systematic Error with Point Turns

In order to observe any error in the wheel tread W, the four-point turns at the corners of the square trajectory can be used. The angular velocity during these turns is

$$\omega(t) = \frac{r(t)}{(W/2)} \frac{l(t)}{(W/2)}.$$

Hence, differentiating with respect to the parameter W, an error δW in W causes an associated error in angular velocity:

$$\delta\omega(t) = -\frac{2r(t)}{W^2}\delta W = \left(-\frac{\delta W}{W}\right)\omega(t) = -\delta\omega_\omega\omega(t).$$

The significance of the minus sign is that an overestimate in wheelbase causes an underestimate in angle of rotation. Also, as noted in the reference, this error is an odd function of angular velocity, so its effects reverse if the direction of rotation is reversed. It also vanishes on straight trajectories so this form of error can only be added to the analysis by reintroducing the previously neglected error integrals during the point turns. During these turns, errors in encoder scale factors also have a potential effect, so they must also be included in the earlier analysis for it to be complete.

A slight change to earlier solutions for differential heading will apply to this case. Consider again, the second set of equivalent errors in eqs. (101) and (104):

$$\begin{bmatrix} \delta V(t) \\ \delta\omega(t) \end{bmatrix}_{DH} dt = \begin{bmatrix} \delta V_\omega\omega(t) \\ \delta\omega_\omega\omega(t) \end{bmatrix} dt = \begin{bmatrix} \delta V_\omega \\ \delta\omega_\omega \end{bmatrix} d\theta$$

$$\begin{bmatrix} \sigma_{vv} & \sigma_{v\omega} \\ \sigma_{v\omega} & \sigma_{\omega\omega} \end{bmatrix}_{DH} dt = \begin{bmatrix} \sigma_{vv}^{(\omega)} & \sigma_{v\omega}^{(\omega)} \\ \sigma_{v\omega}^{(\omega)} & \sigma_{\omega\omega}^{(\omega)} \end{bmatrix} \omega(t)|_{DH}$$

$$dt = \begin{bmatrix} \sigma_{vv}^{(v)} & \sigma_{v\omega}^{(v)} \\ \sigma_{v\omega}^{(v)} & \sigma_{\omega\omega}^{(v)} \end{bmatrix} d\epsilon.$$

On a turn-in-place trajectory, $R(t) = 0$, so the systematic error gradients from eq. (102) are

$$\delta V_\omega = \frac{(\delta r_r - \delta l_l)}{4} W$$

$$\delta \omega_\omega = \left(\frac{\delta r_r + \delta l_l}{2} \right).$$

Adding the additional error due to the wheelbase error gives

$$\delta \omega_\omega = \left(\frac{\delta r_r + \delta l_l}{2} \right) - \left(\frac{\delta W}{W} \right).$$

Now $R(t)|_{DH}$ is infinite on a turn-in-place trajectory as well as a straight one. Hence, the equivalent random error constants on a turn-in-place trajectory are

$$\sigma_{vv}^{(v)}|_{DH} = \frac{\left(\sigma_{rr}^{(r)} + \sigma_{ll}^{(l)} \right)}{4}$$

$$\sigma_{v\omega}^{(v)}|_{DH} = \frac{\left(\sigma_{rr}^{(r)} - \sigma_{ll}^{(l)} \right)}{2W} \tag{142}$$

$$\sigma_{\omega\omega}^{(v)}|_{DH} = \frac{\left(\sigma_{rr}^{(r)} + \sigma_{ll}^{(l)} \right)}{W^2}.$$

The error in wheel radius is assumed to be systematic so it does not affect the variance, although that case can be handled as well. Substituting into the systematic part of eq. (117) gives

$$\delta \underline{x}(\theta)|_{ccw} = \delta \omega_\omega \begin{bmatrix} L\pi \\ -L\pi \\ 2\pi \end{bmatrix} \delta \underline{x}(\theta)|_{cw}$$

$$= \delta \omega_\omega \begin{bmatrix} L\pi \\ L\pi \\ -2\pi \end{bmatrix}. \tag{143}$$

The total error on the entire square trajectory with point turns is the sum of the integrals for the linear and turning portions. Hence the total systematic error due to encoder and wheelbase sources is

$$\delta \underline{x}(t)|_{ccw} = \frac{(\delta r_r - \delta l_l)}{W} \begin{bmatrix} 2L^2 \\ -2L^2 \\ 4L \end{bmatrix}$$

$$\delta \underline{x}(t)|_{cw} = \frac{(\delta r_r - \delta l_l)}{W} \begin{bmatrix} -2L^2 \\ -2L^2 \\ 4L \end{bmatrix}$$

$$+ \left[\left(\frac{\delta r_r + \delta l_l}{2} \right) - \left(\frac{\delta W}{W} \right) \right] \begin{bmatrix} L\pi \\ -L\pi \\ 2\pi \end{bmatrix}$$

$$+ \left[\left(\frac{\delta r_r + \delta l_l}{2} \right) - \left(\frac{\delta W}{W} \right) \right] \begin{bmatrix} L\pi \\ L\pi \\ -2\pi \end{bmatrix}.$$

These are identical to the results in Borenstein and Feng (1995) where the sign convention for positive error in the second term is reversed.

10.3.4. Random Error with Point Turns

The variance due to encoder noises during the turns is also given by the same equation used for the lines (eq. (115)). Integrating over the turn-in-place trajectory gives

$$P(s)|_{ccw} = \sigma_{v\omega}^{(v)}(-LW) \begin{bmatrix} 1 & 0 & 0 \\ 0 & 1 & 0 \\ 0 & 0 & 0 \end{bmatrix}$$

$$+ \sigma_{vv}^{(v)} \left(\frac{\pi}{2} W \right) \begin{bmatrix} 1 & 0 & 0 \\ 0 & 1 & 0 \\ 0 & 0 & 0 \end{bmatrix}$$

$$+ \sigma_{\omega\omega}^{(v)} \begin{bmatrix} \dfrac{\pi}{2} L^2 W & -\dfrac{\pi}{4} L^2 W & \dfrac{\pi}{2} L W \\ -\dfrac{\pi}{4} L^2 W & \dfrac{\pi}{2} L^2 W & -\dfrac{\pi}{2} L W \\ \dfrac{\pi}{2} L W & -\dfrac{\pi}{2} L W & \pi W \end{bmatrix}$$

$$P(s)|_{ccw} = \sigma_{v\omega}^{(v)}(LW) \begin{bmatrix} 1 & 0 & 0 \\ 0 & 1 & 0 \\ 0 & 0 & 0 \end{bmatrix}$$

$$+ \sigma_{vv}^{(v)} \left(\frac{\pi}{2} W \right) \begin{bmatrix} 1 & 0 & 0 \\ 0 & 1 & 0 \\ 0 & 0 & 0 \end{bmatrix}$$

$$+ \sigma_{\omega\omega}^{(v)} \begin{bmatrix} \dfrac{\pi}{2} L^2 W & \dfrac{\pi}{4} L^2 W & -\dfrac{\pi}{2} L W \\ \dfrac{\pi}{4} L^2 W & \dfrac{\pi}{2} L^2 W & -\dfrac{\pi}{2} L W \\ -\dfrac{\pi}{2} L W & -\dfrac{\pi}{2} L W & \pi W \end{bmatrix}.$$

Likewise, the total stochastic error due to both sources is

$$P(s)|_{ccw} = \sigma_{v\omega}^{(v)}(-2L^2 - LW) \begin{bmatrix} 1 & 0 & 0 \\ 0 & 1 & 0 \\ 0 & 0 & 0 \end{bmatrix}$$

$$+ \sigma_{vv}^{(v)} \left(2L + \frac{\pi}{2} W \right) \begin{bmatrix} 1 & 0 & 0 \\ 0 & 1 & 0 \\ 0 & 0 & 0 \end{bmatrix} \tag{145}$$

$$+ \sigma_{\omega\omega}^{(v)} \begin{bmatrix} \dfrac{5}{3} L^3 + \dfrac{\pi}{2} L^2 W - L^3 - \dfrac{\pi}{4} L^2 W & 2L^2 + \dfrac{\pi}{2} L W \\ -L^3 - \dfrac{\pi}{4} L^2 W \dfrac{5}{3} L^3 + \dfrac{\pi}{2} L^2 W & -2L^2 - \dfrac{\pi}{2} L W \\ 2L^2 + \dfrac{\pi}{2} L W - 2L^2 - \dfrac{\pi}{2} L W & 4L + \pi W \end{bmatrix}$$

$$P(s)|_{cw} = \sigma_{v\omega}^{(v)}(2L^2 + LW) \begin{bmatrix} 1 & 0 & 0 \\ 0 & 1 & 0 \\ 0 & 0 & 0 \end{bmatrix}$$

$$+ \sigma_{vv}^{(v)} \left(2L + \frac{\pi}{2} W \right) \begin{bmatrix} 1 & 0 & 0 \\ 0 & 1 & 0 \\ 0 & 0 & 0 \end{bmatrix}$$

$$+ \sigma_{\omega\omega}^{(v)} \begin{bmatrix} \frac{5}{3}L^3 + \frac{\pi}{2}L^2W & L^3 + \frac{\pi}{4}L^2W & -2L^2 - \frac{\pi}{2}LW \\ L^3 + \frac{\pi}{4}L^2W & \frac{5}{3}L^3 + \frac{\pi}{2}L^2W & -2L^2 - \frac{\pi}{2}LW \\ -2L^2 - \frac{\pi}{2}LW & -2L^2 - \frac{\pi}{2}LW & 4L + \pi W \end{bmatrix}.$$

These are the stochastic equivalent of the deterministic UMBmark test. Note that some terms in each element of the state covariance change sign with the direction of rotation whereas others do not. They can be used to calibrate the random component of error evidenced by the spread of the observations over a large number of trials.

10.4. Calibration from Arbitrary Trajectories

While this paper has made much of the difficulty caused by the path-dependent nature of odometry, there are a few advantages to its integral nature. In particular, residuals for each different path to the same terminal point generate independent observations of the sources of error. Therefore, only a single reference point is needed, rather than ground truth for the entire path followed, or the same for a large number of very different paths terminating at different places.

Any number of systematic parameters become particularly convenient to calibrate, in principle, because the burden of ground truth measurement is minimal. The linearized error integrals will be used here as the basis for generating constraint equations. Arbitrary trajectories can be used, but if they are used, it is reasonable to ask why the machinery of the paper should be used rather than, for example, integrating eq. (25) numerically. While this technique will certainly work in some cases, it does require numerical differentiation of an integral with respect to its parameters. The scaling problems encountered in this step may outweigh the simplicity of using eq. (25) whereas the linearized theory requires only numerical integration.

Consider the case of differential heading where the wheel tread and the two wheel radii are to be determined through calibration. The wheel radii errors can be absorbed into the encoder scale errors. After augmenting the inputs with the wheel tread, the inputs are

$$\tilde{\underline{z}} = \begin{bmatrix} V_r & V_l & W \end{bmatrix}.$$

The transition matrix in this case is the same as for integrated heading and is given in eq. (82). The input Jacobian is

$$G(t) = \frac{\partial}{\partial \underline{u}} (\underline{\dot{x}}) \frac{\partial}{\partial \tilde{z}} (\underline{u}) = \begin{bmatrix} c\theta(t) & 0 \\ s\theta(t) & 0 \\ 0 & 1 \end{bmatrix} \begin{bmatrix} \frac{1}{2} & \frac{1}{2} & 0 \\ \frac{1}{W} & -\frac{1}{W} & -\frac{\omega}{W} \end{bmatrix}$$

where

$$\omega = \left(\frac{V_r}{W} - \frac{V_l}{W} \right).$$

This case also illustrates how parameters can be treated in general. The wheelbase was considered an input of equal stature to the wheel velocities. The general solution can now be written as

$$\delta \underline{x}(t) = \underline{IC}_d + \int_0^t \begin{bmatrix} c\theta & -\Delta y(t,\tau) \\ s\theta & \Delta x(t,\tau) \\ 0 & 1 \end{bmatrix} \begin{bmatrix} \frac{1}{2} & \frac{1}{2} & 0 \\ \frac{1}{W} & -\frac{1}{W} & -\frac{\omega}{W} \end{bmatrix}$$

$$\begin{bmatrix} \delta V_r \\ \delta V_l \\ \delta W \end{bmatrix} d\tau.$$

Now, assume that the encoder scale errors are constant so that

$$\begin{bmatrix} \delta V_r(t) \\ \delta V_l(t) \\ \delta W \end{bmatrix} = \begin{bmatrix} \alpha_r V_r(t) \\ \alpha_l V_l(t) \\ \delta W \end{bmatrix}.$$

Define the parameter error vector

$$\delta \underline{p}(s) = \begin{bmatrix} \alpha_r & \alpha_l & \delta W \end{bmatrix}^T.$$

Some manipulation leads to the following final equation

$$\delta \underline{x}(s) = IC(s)\delta \underline{x}(0) + M(s)\delta \underline{p}(s) \qquad (146)$$

where

$$M(s) = M_1(s)M_2(s) + M_3(s)$$

$$IC(s) = \begin{bmatrix} 1 & 0 & -y(s) \\ 0 & 1 & x(s) \\ 0 & 0 & 1 \end{bmatrix} \qquad M_1(s) = \begin{bmatrix} 0 & -y(s) \\ 0 & x(s) \\ 0 & 1 \end{bmatrix}$$

$$M_2(s) = \int \begin{bmatrix} \frac{ds_r}{2} & \frac{ds_l}{2} & 0 \\ \frac{ds_r}{W} & -\frac{ds_l}{W} & \frac{(ds_r - ds_l)}{W^2} \end{bmatrix}$$

$$M_3(s) = \int \begin{bmatrix} c\theta & y(\tau) \\ s\theta & -x(\tau) \\ 0 & 0 \end{bmatrix} \begin{bmatrix} \frac{ds_r}{2} & \frac{ds_l}{2} & 0 \\ \frac{ds_r}{W} & -\frac{ds_l}{W} & \frac{(ds_r - ds_l)}{W^2} \end{bmatrix}.$$

This equation can be written for any number of trajectories for which the uncalibrated trajectory is the basis for the moment calculation and any or all of the residual position and heading errors at a single reference point are used to generate constraints on the unknown parameters.

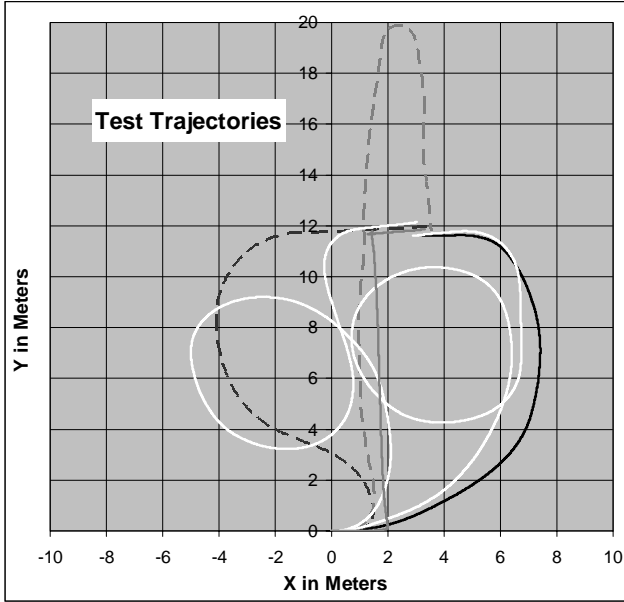Figure 9 shows six such trajectories that were used in this manner.

Fig. 9. Test trajectories for odometry calibration. Six of the 28 trajectories used are shown. All start at the origin with zero heading. All terminate near the point (3,12) with arbitrary heading.
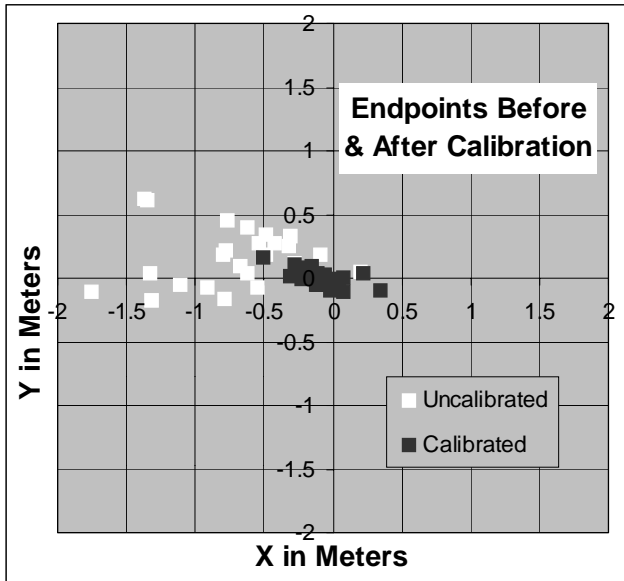

Fig. 10. Residuals both before and after calibration. The white squares represent the computed endpoint residuals for the initial scale factor and wheelbase estimates. The black squares are the results based on solving the overdetermined system of linearized equations.

Zooming in on the correct endpoint, the errors before and after calibration are shown in Figure 10.

The calibrated results were obtained by solving the observation equations by the left pseudo-inverse. Heading residuals were not used due to the need to make extra measurements. The position residuals were taken simply as the difference between the computed endpoint and the known correct answer.

10.5. Optimum Loop Bandwidth in Visual Tracking

The application which originally motivated this work was the vision-based guidance system described in Kelly (2000). In this work the reversibility of systematic error was manifest when the vehicle would reacquire a lock on its position if driven backward after losing lock. A second observation, that optimum performance occurred at precisely 2 Hz update rate, is the subject of this analysis.

Consider the case where a camera is moved at very high speed over a flat surface. A localization algorithm tracks features in a prior appearance model of the scene in order to damp the errors in a odometry system used to provide an estimate of the motion between image acquisitions.

Let the trajectory be a straight line and simplify matters by considering the problem of tracking a single feature in the center of the field of view of the camera. A differential heading system is the basis of the odometry system. The accumulation of position error (for zero initial conditions) is given by eq. (122):

$$P(s) = \sigma_{v\omega}^{(v)} \begin{bmatrix} 0 & s^2/2 & s \\ s^2/2 & 0 & 0 \\ s & 0 & 0 \end{bmatrix}$$

$$+ \sigma_{vv}^{(v)} \begin{bmatrix} s & 0 & 0 \\ 0 & 0 & 0 \\ 0 & 0 & 0 \end{bmatrix} + \sigma_{\omega\omega}^{(v)} \begin{bmatrix} 0 & 0 & 0 \\ 0 & s^3/3 & s^2/2 \\ 0 & s^2/2 & s \end{bmatrix}.$$

For a straight trajectory $R(t)|_{DH}$ is infinite and eq. (105) gives the error gradients as

$$\sigma_{vv}^{(v)} = \frac{\left(\sigma_{rr}^{(r)} + \sigma_{ll}^{(l)}\right)}{4}$$

$$\sigma_{\omega\omega}^{(v)} = \frac{\left(\sigma_{rr}^{(r)} - \sigma_{ll}^{(l)}\right)}{2W}$$

$$\sigma_{v\omega}^{(v)} = \frac{\left(\sigma_{rr}^{(r)} + \sigma_{ll}^{(l)}\right)}{W^2}.$$

Assuming identical error statistics for the two wheels, the solution takes the form

$$P(s) = \sigma_{vv}^{(v)} \begin{bmatrix} s & 0 & 0 \\ 0 & 0 & 0 \\ 0 & 0 & 0 \end{bmatrix} + \sigma_{\omega\omega}^{(v)} \begin{bmatrix} 0 & 0 & 0 \\ 0 & s^3/3 & s^2/2 \\ 0 & s^2/2 & s \end{bmatrix}.$$

The total variance is the accumulated expected squared error radius

$$r^2(s) = \sigma_{xx} + \sigma_{yy} = \sigma_{oo}^{(v)} \left(\frac{s}{4} + \frac{s^3}{3W^2} \right).$$

where $\sigma_{oo}^{(v)} = (\sigma_{rr}^{(r)} + \sigma_{ll}^{(l)})$ is the effective odometry error gradient.

When features are matched a certain amount of random injected error is to be expected. All error is removed when an image is matched except for this noise floor. This error forms the initial conditions for the odometry episode up to the next image match. The initial conditions formula is

$$P_0(s) = \begin{bmatrix} 1 & 0 & -y(s) \\ 0 & 1 & x(s) \\ 0 & 0 & 1 \end{bmatrix} \begin{bmatrix} \sigma_{xx}(0) & \sigma_{xy}(0) & \sigma_{x\theta}(0) \\ \sigma_{xy}(0) & \sigma_{yy}(0) & \sigma_{y\theta}(0) \\ \sigma_{x\theta}(0) & \sigma_{y\theta}(0) & \sigma_{\theta\theta}(0) \end{bmatrix}$$
$$\begin{bmatrix} 1 & 0 & -y(s) \\ 0 & 1 & x(s) \\ 0 & 0 & 1 \end{bmatrix}^T.$$

For a straight trajectory $y(t) = 0$ and $x(t) = s$, so this becomes

$$P_0(s) = \begin{bmatrix} 1 & 0 & 0 \\ 0 & 1 & s \\ 0 & 0 & 1 \end{bmatrix} \begin{bmatrix} \sigma_{xx}(0) & \sigma_{xy}(0) & \sigma_{x\theta}(0) \\ \sigma_{xy}(0) & \sigma_{yy}(0) & \sigma_{y\theta}(0) \\ \sigma_{x\theta}(0) & \sigma_{y\theta}(0) & \sigma_{\theta\theta}(0) \end{bmatrix}$$
$$\begin{bmatrix} 1 & 0 & 0 \\ 0 & 1 & s \\ 0 & 0 & 1 \end{bmatrix}^T.$$

Assuming zero initial cross correlations, this is

$$P_0(s) = \begin{bmatrix} \sigma_{xx}(0) & 0 & 0 \\ 0 & \sigma_{yy}(0) + s^2\sigma_{\theta\theta}(0) & s\sigma_{\theta\theta}(0) \\ 0 & s\sigma_{\theta\theta}(0) & \sigma_{\theta\theta}(0) \end{bmatrix}.$$

For $s \gg 1$ the total variance due to initial conditions is

$$r_0^2(s) = \sigma_{xx}(0) + \sigma_{yy}(0) + s^2\sigma_{\theta\theta}(0).$$

If the initial translational errors are equal and denoted by σ_{vis}^2, then this is

$$r_0^2(s) = 2\sigma_{vis}^2 + s^2\sigma_{\theta\theta}(0).$$

However, $\sigma_{\theta\theta}(0)$ is also related to σ_{vis}^2. Let the initial heading be determined by locating two features separated by an effective image width Λ:

$$\theta = (x_1 - x_2)/\Lambda.$$

The observer Jacobian relates heading error to feature matching error as follows:

$$\delta\theta = \frac{1}{\Lambda} [1 \quad -1] \begin{bmatrix} \delta x_1 \\ \delta x_2 \end{bmatrix} = J\delta\underline{x}$$

$$\sigma_{\theta\theta} = \text{Exp}[\delta\theta\delta\theta^T] = J\text{Exp}[\delta\underline{x}\delta\underline{x}^T]J^T$$

$$\sigma_{\theta\theta} = \frac{1}{\Lambda^2} [1 \quad -1] \begin{bmatrix} \sigma_{11} & 0 \\ 0 & \sigma_{22} \end{bmatrix} \begin{bmatrix} 1 \\ -1 \end{bmatrix} = \frac{2}{\Lambda^2}\sigma_{vis}^2.$$

Therefore, the total variance due to the noise floor is

$$r_0^2(s) = 2\sigma_{vis}^2 \left(1 + \frac{s^2}{\Lambda^2} \right).$$

The total variance due to vision and odometry is

$$r_{tot}^2(s) = \sigma_{oo}^{(v)} \left(\frac{s}{4} + \frac{s^3}{3W^2} \right) + 2\sigma_{vis}^2 \left(1 + \frac{s^2}{\Lambda^2} \right).$$

In order to track a single feature, correlations must be performed for the entire radius of uncertainty. If the pixel size is ρ, and the distance traveled between images is

$$s = V\Delta t$$

then the number of correlations required to search the circular region of uncertainty for a feature is

$$f_{cpu} = \frac{r_{tot}^2(V\Delta t)}{\Delta t} = \frac{\sigma_{oo}^{(v)} \left(\frac{s}{4} + \frac{s^3}{3W^2} \right) + 2\sigma_{vis}^2 \left(1 + \frac{s^2}{\Lambda^2} \right)}{\Delta t}.$$

Figure 11 shows the variation in this expression as the time between images Δt increases. The speed is 0.3 m s^{-1}, pixels are 2.5 mm in size, the wheelbase is 1 m and an image is 0.2 m across. Encoders experience a random error whose variance is 1% of distance and a vision noise floor of one pixel standard deviation is assumed.

A clear minimum exists at an update frequency of 2 Hz. To understand where this comes from, notice that the noise floor (vision) contributes a constant term and a quadratic term whereas odometry contributes linear and cubic terms. A closed-form solution for the extremum requires the roots of the cubic polynomial generated from setting the derivative to zero:

$$\frac{\sigma_{vis}^2}{(\Delta t)^2} = \sigma_{vis}^2 \left(\frac{V^2}{\Lambda^2} \right) + \sigma_{oo}^{(v)} \left(\frac{V^3\Delta t}{3W^2} \right).$$

Given that all terms are positive, it is clear that the growth of the constant part of the noise floor processing as Δt decreases is being balanced by the growth of both the quadratic and cubic terms of f_{cpu} as Δt increases. The optimum update rate is the rate at which both of these effects exactly cancel.

The numeric assumptions used here are not likely to be perfectly accurate. The main point, however, is that an uncorrelated noise floor always implies that a minimum exists and running tracking algorithms as fast as possible is not always the best policy. See Vincze and Weiman (1997) for earlier work on this topic reaching the opposite conclusion when no noise floor is present.
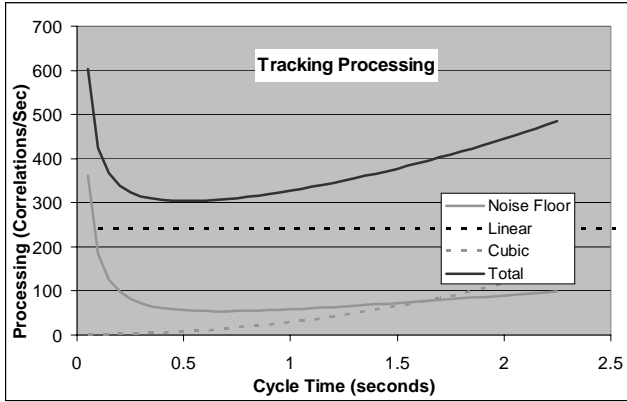
Fig. 11. Visual tracking. Processing requirements experience a minimum around 2 Hz.

10.6. Sensor Comparison

Sensors of disparate modalities can always be compared based on the state error generated on a given trajectory. In the case of gyros and differential odometry, a relationship was derived earlier which effects a more direct comparison. Consider again the systematic equivalent integrated heading error sources for a given differential heading setup. From eq. (102):

$$\delta V_v(t) = \left\{ \left(\frac{\delta r_r + \delta l_l}{2} \right) + \frac{(\delta r_r - \delta l_l)}{4R(t)} W \right\}$$

$$\delta \omega_v(t) = \left\{ \frac{(\delta r_r - \delta l_l)}{W} + \left(\frac{\delta r_r + \delta l_l}{2R(t)} \right) \right\}.$$

Differential heading will be most competitive with a gyroscope when the curvature is zero and the second terms in the second line vanish. Under these conditions, the equivalent gyro bias is

$$\delta \omega(t) = \delta \omega_v(t) V(t) = \frac{(\delta r_r - \delta l_l)}{W} V(t).$$

The motion-dependent nature of differential heading implies that if time is not important, the velocity can always be reduced enough to beat the performance of any gyro. However, in a realistic context, the velocity needs to be on the order of 1 m s^{-1} and the wheelbase is also of the order of 1 m. Equating to a gyro bias gives

$$(\delta r_r - \delta l_l) = \delta \omega(t) \frac{W}{V} = \delta \omega(t).$$

Hence the difference in encoder scale errors corresponds to an equivalent gyro bias. On the presumption that the encoder scale errors can be calibrated to a residual 0.5%, the difference between the residual errors cannot exceed 1%. Solving for the equivalent residual gyro bias leads to

$$\delta \omega(t) = (\delta r_r - \delta l_l) = 1\% = 0.01 \text{ rads s} = 2063 \text{ deg h}^{-1}.$$

While this level of performance (0.6 deg s^{-1}) is comparable to the best contemporary MEMS gyros, contemporary fiber optic gyros exceed it by several orders of magnitude. On this basis alone, such gyros can be expected to significantly outperform differential heading in practice even before accounting for their relative immunity to floor irregularities.

11. Extensions

This section sketches some ways in which the theory can be extended.

11.1. 3D Odometry: Strapped Down Integrated Attitude and Heading Configuration

Given the ease with which 2D odometry yielded to linearized analysis, it is natural to wonder whether 3D odometry can be analyzed similarly. 3D odometry can be accomplished with indications of the attitude and heading of the vehicle (or their derivatives) as well as its translational speed.

Let axes be assigned to the body fixed frame according to the SAEJ670e convention: x forward, y to the right, z down. Let the world fixed frame be coincident with the body frame when the pose of the vehicle is zero in all six degrees of freedom. Let a z–y–x Euler angle sequence be used. Then, the rotations which move the earth-fixed frame of reference into coincidence with the vehicle-fixed frame is to rotate first by the yaw angle ψ around the z-axis, then by the pitch angle θ around the new y-axis, and then by the roll angle ϕ around the new x-axis.

Let there be three strapped down gyroscopes oriented along the three axes of the body frame reading the three components of angular velocity $\bar{\omega}$. To simplify matters, assume they indicate angular velocity relative to the world frame (rather than an inertial frame). Let ψ denote yaw, θ denote pitch, and ϕ denote roll. Under these assumptions, the equations of 3D odometry are

$$\frac{d}{dt} \begin{bmatrix} x \\ y \\ z \\ \phi \\ \theta \\ \psi \end{bmatrix} = \begin{bmatrix} V c\psi c\theta \\ V s\psi c\theta \\ -V s\theta \\ \omega_x + t\theta(\omega_y s\phi + \omega_z c\phi) \\ \omega_y c\phi - \omega_z s\phi \\ \frac{1}{c\theta}(\omega_y s\phi + \omega_z c\phi) \end{bmatrix}. \tag{147}$$

The Jacobian of this system is

$$F = \begin{bmatrix} 0 & 0 & 0 & 0 & c\psi \dot{z} & -\dot{y} \\ 0 & 0 & 0 & 0 & s\psi \dot{z} & \dot{x} \\ 0 & 0 & 0 & 0 & -V c\theta & 0 \\ 0 & 0 & 0 & t\theta\dot{\theta} & \frac{\dot{\psi}}{c\theta} & 0 \\ 0 & 0 & 0 & -c\theta\dot{\psi} & 0 & 0 \\ 0 & 0 & 0 & \frac{\dot{\theta}}{c\theta} & t\theta\dot{\psi} & 0 \end{bmatrix} \tag{148}$$

where $t\theta$ denotes the tangent.

It turns out that the transition matrix for this system is very difficult to derive. Consider trying to use eq. (59). Recall the definition:

$$R = \int_{\tau}^{t} F(\zeta)d\zeta.$$

Use of this technique for the transition matrix requires that

$$FR = RF. \tag{149}$$

Taking, for example, the top element of the fifth column of both matrices leads to

$$\dot{\psi}\tan(\theta)\int_{\tau}^{t}\dot{y}(\zeta)d\zeta \overset{?}{=} \dot{y}\int_{\tau}^{t}\dot{\psi}\tan\theta(\zeta)d\zeta.$$

Clearly, these are not equal in general so eq. (59) cannot be used. This has occurred because strapping the gyros down makes the orientation rates depend on the orientation, breaking the intuitive rule stated earlier of unit depth dependences. More generally, the technique of Section 6.4 can be used.

By analogy to Section 7.2.4, the transition matrix can be derived by differentiating the kinematic relationships between coordinate frames corresponding to times 0, t, and τ. The homogeneous transform relating two frames in arbitrary position using the SAE convention is

$$T = \begin{bmatrix} c\psi c\theta & c\psi s\theta s\phi - s\psi c\phi & c\psi s\theta c\phi + s\psi s\phi & x \\ s\psi c\theta & s\psi s\theta s\phi + c\psi c\phi & s\psi s\theta c\phi - c\psi s\phi & y \\ -s\theta & c\theta s\phi & c\theta c\phi & z \\ 0 & 0 & 0 & 1 \end{bmatrix}.$$

As in the earlier example, the pose of the endpoint can be written as the product:

$$T_t^0 = T_\tau^0 T_t^\tau.$$

If we partition the state vector into translational and rotational components thus:

$$\underline{x} = \begin{bmatrix} \underline{r}^T & \underline{\Omega}^T \end{bmatrix}^T \quad \underline{r} = \begin{bmatrix} x \\ y \\ z \end{bmatrix} \quad \underline{\Omega} = \begin{bmatrix} \phi \\ \theta \\ \psi \end{bmatrix}.$$

Then, the Jacobian is composed of four elements:

$$\frac{\partial \underline{x}(t)}{\partial \underline{x}(\tau)} = \begin{bmatrix} \dfrac{\partial \underline{r}(t)}{\partial \underline{r}(\tau)} & \dfrac{\partial \underline{r}(t)}{\partial \underline{\Omega}(\tau)} \\ \dfrac{\partial \underline{\Omega}(t)}{\partial \underline{r}(\tau)} & \dfrac{\partial \underline{\Omega}(t)}{\partial \underline{\Omega}(\tau)} \end{bmatrix}.$$

Two of these elements are trivial:

$$\frac{\partial \underline{r}(t)}{\partial \underline{r}(\tau)} = I \quad \frac{\partial \underline{\Omega}(t)}{\partial \underline{r}(\tau)} = 0.$$

The other two are quite complicated but they should be within the reach of symbolic mathematics packages. For example:

$$\frac{\partial x(t)}{\partial \phi(\tau)} = (c\psi s\theta c\phi + s\psi s\phi)_\tau^0 y_t^\tau$$

$$+ (-c\psi s\theta s\phi + s\psi c\phi)_\tau^0 z_t^\tau.$$

An alternative route to computing the partials of angles with respect to angles would be to use quaternions. When the explicit formula for the transition matrix is available, it is already clear that new 3D Fourier moments will arise from terms like those in the last equation.

11.2. 3D Odometry: Stabilized Integrated Attitude and Heading Configuration

Suppose that the gyros are mounted on a platform stabilized to maintain its initial attitude with respect to the earth. The gimbal rates $\vec{\rho}$ required to stabilize the platform are a direct readout of the Euler angle rates. Then the system dynamics are

$$\frac{d}{dt}\begin{bmatrix} x \\ y \\ z \\ \phi \\ \theta \\ \psi \end{bmatrix} = \begin{bmatrix} Vc\psi c\theta \\ Vs\psi c\theta \\ -Vs\theta \\ \rho_x \\ \rho_y \\ \rho_z \end{bmatrix}. \tag{150}$$

The system Jacobian is

$$F = \begin{bmatrix} 0 & 0 & 0 & 0 & c\psi \dot{z} & -\dot{y} \\ 0 & 0 & 0 & 0 & s\psi \dot{z} & \dot{x} \\ 0 & 0 & 0 & 0 & -Vc\theta & 0 \\ 0 & 0 & 0 & 0 & 0 & 0 \\ 0 & 0 & 0 & 0 & 0 & 0 \\ 0 & 0 & 0 & 0 & 0 & 0 \end{bmatrix}. \tag{151}$$

Now $FR = RF = 0$ and the transition matrix is much easier to obtain. Direct heading can be expected to behave similarly.

11.3. Discrete Time Error Propagation

The availability of the exact continuous time transition matrix renders the conversion to discrete time fairly straightforward. Let the subscript k be used to denote function evaluation at time step t_k.

In the discrete time case, the perturbative state equations are of the form

$$\underline{x}_{k+1} = F_k \underline{x}_k + G_k \underline{u}_k$$

for which the general solution is

$$\underline{x}_n = \Phi_{n,0}\underline{x}_0 + \sum_{k=0}^{n} \Phi_{n,k+1} G_k \underline{u}_k.$$

The transition matrix between any two times is computed by simply substituting the times into the continuous form:

$$\Phi_{n,k} = \Phi(t_n, t_k).$$

11.4. Generic Error Models

So far, the error models that have been assumed have been relatively straightforward and motivated by intuition and experience. However, the technique of substituting a power series into an integro-differential equation has been known for centuries.

Here, the importance of this matter is that the Taylor series is convergent in most practical situations. If there is reason to believe that, for example, a particular source of error $\varepsilon(t)$ is a complicated function of velocity, it can be written as

$$\varepsilon(t) = a + bV(t) + cV^2(t) + dV^3(t) + \dots . \quad (152)$$

When enough observations are available, such models can be calibrated to determine the coefficients. The technique is not limited to polynomials, any parametrized relationship can be used. Likewise, dependence on any combination of states and inputs can be modeled in principle.

12. Validation

As a linear approximation, the results of earlier sections can be expected to represent the dominant behavior of odometry error propagation up to the point where neglected higher-order terms become significant. This section uses numerical techniques to validate the linearized theory by evaluating the significance of these higher-order terms on a representative example.

Error propagation results were verified by comparing the linearized solutions of the article with an exact nonlinear numerical solution for both systematic and random errors. The integrated heading case was chosen for the simulation. The input error characteristics were as shown in Table 2.

These models represent a systematic scale error of 5% on velocity and a motion-dependent random walk stochastic velocity error of equal standard deviation. A systematic gyro bias of 30 deg h^{-1} is used as well as a bias stability of equal standard deviation.

Table 2. Error Sources for Monte Carlo Analysis

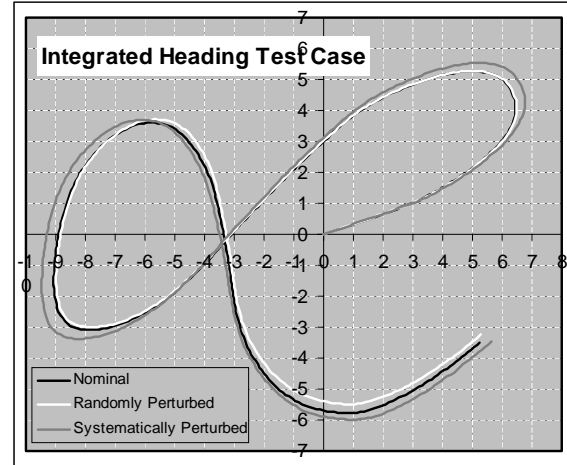| Error Source	Deterministic	Random
Linear Velocity	$\delta V = \alpha V$ $\alpha = 0.05$	$\sigma_v = \delta V$
Angular Velocity	$\delta \omega = b$ $b = 30$ deg h^{-1}	$\sigma_\omega = b$

Fig. 12. Nonlinear numerical solution on a test trajectory. Effects of both systematic and random error are shown. The systematic error is initially larger but mostly cancels on the closed loop. The random error is more subdued but more persistent.
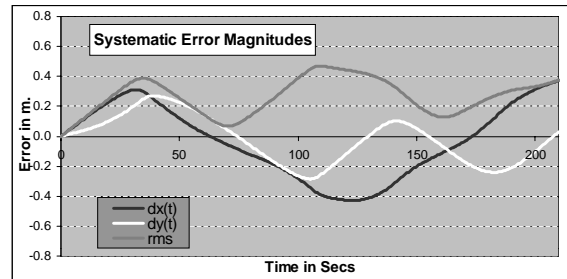

Fig. 13. Systematic error magnitudes. The loop closes at the last point where both error curves cross. At this point, only the incoming initial error and the accumulated gyro error on the loop remains.

Such error magnitudes are considerably larger than might be expected in a practical situation. The intention here is both to stress the linearity assumption and to provide a common error magnitude for both systematic and random sources which is large enough to be noticeable in Figures 12–15.

In the systematic case, straightforward numerical quadrature can be used to integrate the nonlinear dynamics in both the perturbed and unperturbed case and the difference between the two is obtained as the exact nonlinear solution within the limits of time discretization. Computing exact nonlinear dynamics for stochastic systems is not so straightforward. Monte Carlo simulation was used to generate a large number of separately and randomly perturbed solutions to the system dynamics whose statistics could then be computed and compared with the linearized solution of the article.
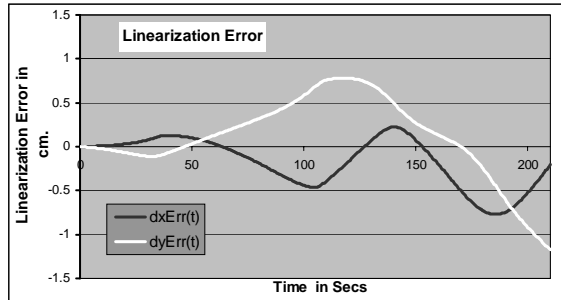
Fig. 14. Linearization error. Linearized error dynamics are accurate to 3% even in the presence of unrealistically large encoder and gyro errors.
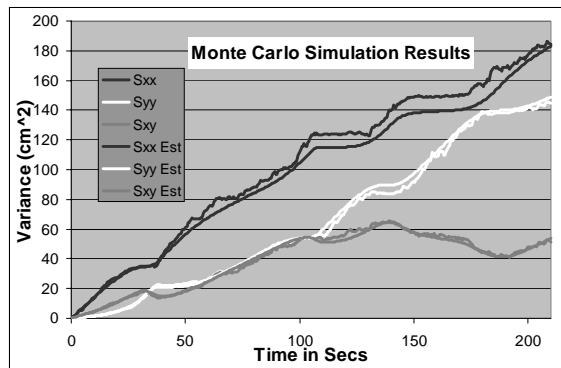

Fig. 15. Monte Carlo simulation compared to theory. Agreement of the full nonlinear solution with theory is excellent. Note how the two translational variances vary symmetrically about a steady growth curve.

Roughly 500,000 independent, unbiased, unit variance Gaussian random variables were first generated. Half were designated for linear velocity error $\delta V(t)$ and the other half for angular velocity error $\delta \omega(t)$. Each set was divided into 250 discrete time random signals which were then scaled appropriately and presented to the nonlinear system as random corruptions to the nominal inputs.

Figure 12 illustrates the result of nonlinear simulation; an arbitrary trajectory chosen to contain a loop but exhibiting no particular symmetry. The velocity for the test is 0.25 m s^{-1}, the total time is 210 s and the time step is 0.5 s.

While there is a single systematic result to plot, only one representative of the 250 randomly perturbed trajectories is shown. Due to the tendency of random error to cancel in the short term, the effect of systematic error is locally more dramatic when compared to a random error. However, systematic error may cancel in the long term due to path independence

or symmetry, while decreases in random error over the long term are less likely.

The effect of the systematic velocity scale error is evident in the increase in error magnitude with the radius from the origin. As predicted by theory, substantial accumulated systematic errors in the far left vanish when the loop closes. For random error, the overall growth rate is more subdued but it nonetheless accumulates to nontrivial levels over time, particularly at the end of the trajectory.

The magnitude of systematic error is presented in Figure 13. On this scale, the difference between linearized and nonlinear error propagation in not detectable. Angular error is omitted because it is linear by construction. The point of loop closure is the last place where both translational error curves cross.

The difference between linearized and nonlinear error is shown in Figure 14.

Clearly, the linearized solution is an excellent approximation for errors of this magnitude. Throughout the test, the difference between exact and linearized solutions never exceeds 1 cm or 3% of the actual error magnitude. This result validates the systematic part of eq. (87).

The results of the Monte Carlo simulation are provided in Figure 15 for the translational variances and covariances. Rotational variance is linear by construction and translational–rotational covariances agree similarly with theory. The agreement between theory and simulation is excellent. Note how the two translational variances exhibit conservation behavior by varying symmetrically about an average steady growth curve.

Overall, three classes of error can be expected in the stochastic case: linearization, discretization, and sampling error. The first two classes have been demonstrated to be relatively small by the systematic error results. These curves show that for a sample size of 250 pairs of input random processes, the sample variance of the state covariance matrix tracks the linearized theoretical population variance quite well. This result validates stochastic part of eq. (87).

13. Summary

The goal of this paper has been to discover and understand the major behaviors of odometry error propagation. Linear systems and optimal estimation theory have provided all of the necessary tools. All of the most important interpretation of the mathematical results has been reserved for this section.

13.1. Dynamics

Odometry is distinct from both inertial guidance and triangulation in fundamental ways. Odometry is dead reckoning; solutions and their errors propagate according to nonlinear differential equations whose solutions are integrals.

While odometry is nonlinear it is often homogeneous in its inputs. The fact that the odometry solution stops moving

when the inputs are nulled is closely related to the facts that error propagation also stops when motion stops, that certain systematic errors cancel on closed trajectories, and that some are reversible.

The key to the direct application of linear systems theory to error propagation is to linearize both the system dynamics and the observer equation and substitute the observer into the dynamics. The result is referred to here as the "forced dynamics" formulation.

13.2. Solution Basis

Once the equations are linearized, the general solutions for both systematic and random error propagation can be written immediately in terms of the transition matrix, which is known to exist but may not be easy to find or express in closed form. As a linear solution, the output is the sum of a path-independent response to initial conditions and a generally path-dependent response to the input history. In both the systematic and random error cases, both elements of the response may exhibit zeros and extrema and neither is necessarily monotone.

The input response can be expressed as a sum of a set of vector and matrix-valued basis functions which describe the response of pose error to each individual source of input sensor error. This solution basis comprises a set of integral transforms of the inputs where the convolution kernel is derived from the columns of the product of the transition matrix and the input Jacobian. The basis also supplies the canonical form of many error propagation behaviors. When errors are of simple forms, the integral transforms take the form of moments of the reference trajectory. In this way, linear systems theory provides the explicit relationship between the shape of the path followed and the projection of sensor errors onto solution errors.

13.3. Error Propagation Behaviors

These moments can be tabulated for specific trajectory shapes and used like tables of moments of inertia or Laplace transforms. They generate the interesting behaviors of error dynamics. Two classes of moments are the spatial moments and the Fourier moments. The spatial moments are simply moments of arc evaluated about the endpoint. The Fourier moments are essentially the Fourier series coefficients. Spatial moments apply to angular velocity errors and Fourier moments apply to linear velocity errors. Systematic error tends to propagate with the first-order moments and random error with both first-order and second-order moments. Linear and angular biases tend to propagate in a time-dependent manner whereas scale errors generate motion-dependent behavior.

The first-order Fourier moments are path-independent whereas the second-order moments are monotone. Patterns of systematic error behavior correspond to related patterns of random error behavior. Thus, systematic velocity scale error cancels on closed trajectories and random velocity error grows monotonically in total variance although error ellipses may rotate over time. The first spatial moments vanish at the centroid of the trajectory and the second moments reach extrema at the same places. Random pose error due to angular velocity indications (such as gyros) is not monotone.

Thus, odometry usually performs well at the point of closure of closed symmetric paths for fundamental reasons. Good gyros will tend to outperform differential heading odometry. On a symmetric figure 8 trajectory with the origin at the center, the effects of both velocity scale error and systematic gyro bias will vanish. Accordingly, closed and/or symmetric trajectories may or may not be good choices for calibrating errors, depending on what sensitivities are being emphasized or suppressed.

13.4. Closed-Form Dynamics

In addition to being a nonlinear, input homogeneous system, odometry is also often in echelon form with state variable coupling that is no more than unit depth. This structure leads to a system Jacobian which is strictly upper rectangular, which, in turn, leads to a rapidly terminating exponential series for the transition matrix as well as the right to use the series in the first place.

The general solution for linearized dynamics is converted to specific solution for a given problem by making three choices: the form of odometry determines the form of input transition matrix, the reference trajectory fixes its value, and the error inputs drive the linearized system with respect to the reference trajectory.

Different forms of odometry have different system and input Jacobians. As a result, they have different input transition matrices and different forms of the general solution. Different forms are equivalent when only the input Jacobian and/or observer differs. Differential heading odometry, for example, is just a form of integrated heading with an input observer. The same general solution applies and a given set of differential heading inputs and input errors can be converted using the observer to equivalent inputs and input errors for integrated heading. Consequently, it is sometimes possible to convert one sensor package to another equivalent one composed of different sensors.

In a linearized solution, the Jacobians are not updated to reflect the errors in the assumed reference trajectory that become known as the solution is computed over time. This means that errors are treated as if they do not compound (but not as if they do not accumulate) and the solution integrals can therefore be understood on an intuitive level as the accumulation of the suitably scaled effects of the input error history.

13.5. Applications

The theory can be applied to a large number of applications and extended to 3D. Variational methods can be used to

determine trajectories of extreme error. The trace of the trajectory moment matrix is the logical performance index for random error. Using this, it is easy to show that the trajectory minimizing accumulated error when traveling between any two points is a straight line.

The theory applies to any form of odometry for which the transition matrix can be found, for any trajectory or error model. For example, lateral wheel slip can be shown to propagate (like a gyro scale error) according to spatial rotation moments.

A clear application is the calibration of both systematic and random error models by using the linearized error equations as models to be calibrated. In the case of the University of Michigan odometry benchmark, the equivalent stochastic calibration method can be derived easily.

Tracking problems can be analyzed with the theory to both show that an optimum finite update rate exists and extract its value for given error magnitudes.

14. Conclusions

It has not been the purpose here to demonstrate that commonly used models of error propagation are sufficiently representative of reality. The entire field of optimal estimation, including Kalman filtering, routinely uses linear models, assumptions of decorrelation, etc. The main purpose here has been to show that the associated models can be solved in closed form and that those solutions generate important insights into the general case.

In addition to their pedagogic value, these results can be used:

- in design to determine acceptable levels of sensor error, or determine optimal approaches to error compensation;

- in analysis to predict performance of a given design;

- in calibration and evaluation to accentuate or attenuate response to individual error sources;

- in operation to plan trajectories in order to minimize exposure to specific error sources.

Trajectory moments figure prominently in the analytical theory of odometry error propagation. Propagation is essentially determined by a combination of the moments of arc and the Fourier coefficients of the vehicle trajectory. Tables of such moments for given trajectories can encapsulate solutions to estimation problems in a manner analogous to the use of the Laplace transform in control, the Fourier transform in signal processing, or the moment of inertia in dynamics.

As exemplified here, analytic expressions are important tools in the development of theory. The present results enable the symbolic application of linear systems theory, optimal control, calculus of variations, etc., to any application which attempts to account in some way for odometry error propagation.

References

Borenstein, J., and Feng, L. 1995. Correction of systematic odometry error in mobile robots. In *Proceedings of IROS 95*, Pittsburgh, PA, August 5–9.

Britting, K. 1971. *Inertial Navigation System Analysis*, Wiley, New York.

Bona, B. E., and Smay, R. J. 1966. Optimum reset of ship's inertial navigation system. *IEEE Transactions on Aerospace Electrical Systems*, 2(4):409–414.

Brogan, W. L. 1974. *Modern Control Theory*, Quantum, New York.

Brown, R. C., and Hwang, P. 1996. *Introduction to Random Signals and Applied Kalman Filtering*, Wiley, New York.

Chong, K. S., and Kleeman, L. April 1997. Accurate odometry and error modeling for a mobile robot. In *Proceedings of ICRA 1997*, Albuquerque, NM.

Nettleton, E. W., Gibbens, P. W., and Durrant-Whyte, H. F. 2000. Closed form solutions to the multiple platform simultaneous localization and map building (SLAM) problem. In *Proceedings of AeroSense 2000*, Orlando, FL.

Durrant-Whyte, H. March 1987. Uncertain geometry in robotics. In *Proceedings of ICRA 1987*, Raleigh, NC, pp. 851–856.

Gelb, A., editor. 1974. *Applied Optimal Estimation*, MIT Press, Cambridge, MA.

Kelly, A. 2000. Mobile robot localization from large scale appearance mosaics. *International Journal of Robotics Research* 19(11):1104.

Maybeck, P. S. 1982. *Stochastic Models, Estimation, and Control*, Academic Press, New York.

Milliken, R. J., and Zoller, C. J. 1978. Principle of operation of NAVSTAR and system characteristics. *Navigation* 25(2):95–106.

Pinson, J. C. 1963. Inertial guidance for cruise vehicles. In *Guidance and Control of Aerospace Vehicles*, C. T. Leondes, editor, McGraw-Hill, New York, Chap. 4.

Smith, R. C., and Cheeseman, P. 1986. On the representation and estimation of spatial uncertainty. *International Journal of Robotics Research* 5(4):56–68.

Stengel, R. 1994. *Optimal Control and Estimation*, Dover, New York.

Vincze, M., and Weiman, C. 1997. On optimizing tracking performance for visual servoing. In *Proceedings of ICRA 1997*, Albuquerque, NM.

Wang, C. M. 1988. Location estimation and uncertainty analysis for mobile robots. In *Proceedings of the IEEE Conference on Robotics and Automation (ICRA 88)*, Philadelphia, PA, pp. 1230–1235.